1990ApJ...359..164T

THE ASTROPHYSICAL JOURNAL, 359:164–175, 1990 August 10
© 1990. The American Astronomical Society. All rights reserved. Printed in U.S.A.

STRUCTURE AND EVOLUTION OF IRRADIATED ACCRETION DISKS. I. STATIC THERMAL EQUILIBRIUM STRUCTURE

Y. TUCHMAN,[1] S. MINESHIGE,[2] AND J. C. WHEELER
Astronomy Department, University of Texas at Austin
Received 1989 October 2; accepted 1990 February 12

ABSTRACT

The thermal equilibrium structure of externally irradiated accretion disks is investigated. We assume that the irradiation flux is thermalized in the photosphere of the disk. The vertical structure of the disk can then be calculated by changing the surface boundary conditions. The response of the disk structure to the irradiation is totally different for radiative disks and for convective disks. For radiative disks, only the surface layer is heated by the irradiation, and there is practically no change in the internal structure. In the convective disks, however, the heat of irradiation can penetrate deeply into the disk, and thus the temperature increases at every depth. For a sufficiently strong irradiation with $T_{\rm irr} > 10{,}000$ K, where the irradiation flux is $F_{\rm irr} \equiv \sigma T_{\rm eff}{}^4$, the disk is completely stabilized against thermal instabilities of the sort invoked to explain dwarf novae. For moderately strong irradiation $T_{\rm irr} \sim 6000$ K, however, there is still an unstable branch in the thermal equilibrium curve, although the difference in the temperature between the hot stable state and the cool stable state is less than that in nonirradiated disks. A simplified analytic model is presented to understand the effects of irradiation on the vertical structure of the disks.

It is shown that in typical soft X-ray transients such as Aql X-1, Cen X-4, and A0620−00, irradiation can be completely neglected in quiescence; the disk is thus unstable against the dwarf-nova type instability. At maximum light, however, irradiation may suppress the instability. It is suggested that the 300 day modulation of the soft X-ray luminosity in Cyg X-1 might be caused by the thermal instability. Possible mechanisms to initiate the downward thermal transition are discussed.

Subject headings: stars: accretion — stars: dwarf novae — X-rays: binaries

I. INTRODUCTION

Accretion disks have two possible heating sources: viscous heating generated in the body of the disk and surface heating by irradiation from the central compact object and by the inner part of the disk. The standard accretion disk model is constructed by equating the viscous heating rate with the radiative cooling rate (see the review by Pringle 1981). For a given mass transfer rate into the disk, the effective temperature distribution is uniquely determined regardless of the viscosity prescriptions (Lynden-Bell and Pringle 1974). When the viscosity parameter, α, is assigned, one can obtain a detailed structure for the disk, such as the surface density, the central temperature, and the thickness as functions of radius (Shakura and Sunyaev 1973).

According to the disk instability model (Osaki 1974), accretion disks in dwarf novae have two different thermally stable states: in quiescence matter is stored in the disk, and in outbursts matter is quickly released to flow inward. Meyer and Meyer-Hofmeister (1981, 1982) calculated the vertical structure of accretion disks using realistic opacities and including convective energy transport in the vertical direction. For typical parameters relevant to dwarf nova disks, they found S-shaped thermal equilibrium curves in the effective temperature–surface density plane, in which the middle branch with negative slope was shown to be thermally unstable due to the partial ionization zones of hydrogen and helium and the resultant convection (see also Hōshi 1979; Smak 1982; Faulkner, Lin, and Papaloizou 1983, hereafter FLP; Mineshige and Osaki 1983; Cannizzo and Wheeler 1984). With this S-shaped thermal equilibrium curve, steady accretion is no longer possible. The accretion disk inevitably alternates between the hot state with $T_{\rm eff} \geq 10^4$ K ($T_{\rm eff}$ is the effective temperature), where hydrogen and helium are completely ionized, and the cool state with $T_{\rm eff} \ll 10^4$ K, where the hydrogen and the helium are recombined. Time-dependent calculations of the thermal instability in dwarf nova disks have been executed by many groups (Papaloizou, Faulkner, and Lin 1983; Smak 1984; Meyer and Meyer-Hofmeister 1984*a*; Lin, Papaloizou, and Faulkner 1985; Mineshige and Osaki 1985; Cannizzo, Wheeler, and Polidan 1986; Mineshige 1986; Pringle, Verbunt, and Wade 1986).

Soft X-ray transients are one subgroup of low-mass X-ray binaries. Their outbursts are in many respects similar to those of dwarf novae (see van Paradijs and Verbunt 1984; Priedhorsky and Holt 1987). It is thus natural to expect that the same mechanism as dwarf novae is operating also in soft X-ray transients (Cannizzo, Wheeler, and Ghosh 1985), but there is a basic difference between these two types of systems. In cataclysmic variables, where accretion disks surround white dwarfs, the external heating may be neglected, whereas in low-mass X-ray binaries, where the central neutron star and the inner regions of the disk release about 10^3 times more radiation than the white dwarf in dwarf novae, the external heating cannot be ignored. The thermal structure of the disk will be significantly altered by the presence of the strong X-ray flux (Shakura and Sunyaev 1973; Hayakawa 1981). The heated surface might expand, form an optically thin corona, and may escape from the disk as a wind (Begelman, McKee, and Shields 1983). As a result, the thermal instability of the dwarf nova type might be suppressed (Meyer and Meyer-Hofmeister 1984*b*;

[1] Permanent address: Department of Physics, Hebrew University.
[2] Also at Institute for Fusion Studies, University of Texas at Austin.

© American Astronomical Society • Provided by the NASA Astrophysics Data System

1990ApJ...359..164T

Saito 1989). If this were true in general, the thermal instability model would not be relevant for soft X-ray binaries. Hameury, King, and Lasota (1986) proposed an alternative model, in which the secondary star surface suffers a mass-transfer burst instability and is responsible for outbursts in soft X-ray transients (see also Hameury, King, and Lasota 1987, 1988).

The effect of irradiation is therefore a crucial factor for the disk instability model for soft X-ray transients. Assuming X-ray irradiation to be small, Huang and Wheeler (1989) and Mineshige and Wheeler (1989) calculated the propagation of disk thermal instabilities as a model for the possible black hole candidate A0620−00. This assumption is justified in quiescence, because at that phase the X-ray luminosity is very low; below the detection limit of $L_x \sim 10^{32}$ ergs s^{-1} (Long, Helfand, and Grabelsky 1981).

In this paper, we focus on modifications of the thermal equilibrium curves caused by the existence of external irradiation. The dynamical behavior of irradiated disks will be investigated in the next paper (Mineshige, Tuchman, and Wheeler 1990, hereafter Paper II). The plan of this paper is as follows. The method of calculation is explained in § II. It is basically the same as that employed to integrate stellar envelopes. The results concerning the thermal equilibrium curves and the temperature distribution in the vertical direction of the disk are illustrated in § III. To understand the numerical results, we construct a simple analytical model in § IV. The final section is devoted to discussion of observational implications and conclusions.

II. METHODS OF CALCULATION

In this section, we present the method of calculating the vertical structure of an irradiated disk following a modified version of the conventional method used for stellar envelopes (e.g., see Tuchman, Sack, and Barkat 1978).

The basic equations, based on the α model, are as follows:

Mass conservation,

$$\frac{d\Sigma_z}{dz} = 2\rho \,, \tag{1}$$

where Σ_z is the integrated surface density from the central plane of the disk to the vertical height, z, and ρ is the local density. For momentum conservation, we assume hydrostatic balance neglecting the self-gravity of the disk,

$$\frac{dP}{dz} = -g\rho \equiv -\frac{GM}{r^3} z\rho \,, \tag{2}$$

where P is the local pressure, g is the vertical component of the gravitational force induced by a central star of mass M, and r is the radius of the disk. For energy conservation within the disk, we assume a local energy balance between the net energy losses carried by the flux F_z and the viscous heating rate,

$$\frac{dF_z}{dz} = \frac{3}{2}\alpha P\Omega \,, \tag{3}$$

where α is the viscosity parameter (Shakura and Sunyaev 1973) and $\Omega = (GM/r^3)^{1/2}$. In this paper we assume a constant value of $\alpha = 0.1$. F_z includes radiative and convective transfer processes. The radiative flux is given by:

$$F_r = \frac{4ac}{3}\frac{T^4}{\kappa\rho}\frac{f_1(\tau)}{\lambda_p}\nabla \,, \tag{4}$$

and the convective flux is calculated according to the recipe given by Spiegel (1963),

$$F_c = \left(\frac{Q}{2}\right)^{1/2}\frac{1}{4}\rho T C_p (g\lambda_p)^{1/2}\left(\frac{\Lambda}{\lambda_p}\right)^2 (\nabla - \nabla')^{3/2} \,, \tag{5}$$

where $f_1(\tau)$ is a correction factor of order unity, which is derived based on the discrete ordinate approximation of the fourth order (see Appendix), κ is the local Rosseland mean opacity, $\lambda_p (\equiv P/\rho g)$ is the pressure scale height, C_p is the specific heat at constant pressure, Λ is the mixing length parameter, and ∇ and ∇' are the temperature gradients for the ambient material and for the convective element, respectively (see Cox and Guili 1968):

$$Q = 1 - \left(\frac{\partial \ln \mu}{\partial \ln T}\right)_P \,, \tag{6a}$$

$$\nabla \equiv \frac{d\ln T}{d\ln P} \,, \tag{6b}$$

$$\nabla' \equiv \left(\frac{d\ln T}{d\ln P}\right)_{\rm conv} \,, \tag{6c}$$

where μ is the mean molecular weight. The mixing length Λ is chosen to be one pressure scale height. The optical depth through the disk is defined by:

$$\frac{d\tau}{dz} = \kappa(\rho, T)\rho \,. \tag{7}$$

The equation of state was taken as the sum of contributions of the radiation, and ideal gas of electrons, H_2, H_2^+, H, H^-, H^+, He^+, and He^{++}, where the abundances were determined by a solution of the Saha equation. Opacities were adopted from Cox and Stewart (1970) for a Population I composition ($X = 0.70$, $Y = 0.27$). In addition, we include the contribution from water molecules in the way suggested by Paczyński (1969).

For a given value of the external (surface) temperature, $T_{\rm ex}$, the external flux (flux from the interior to the surface), $F_{\rm ex}$, is calculated by:

$$F_{\rm ex} = \frac{8\sigma T_{\rm ex}^4}{3f_2(\tau_{\rm ex})} - F_{\rm irr} \,, \tag{8}$$

where the first term on the right-hand side represents the outgoing flux from the surface, $F_{\rm irr}$ denotes the incident flux into the surface layer by external heat sources, and $f_2(\tau)$ is a correction factor of order unity (see Appendix). For convenience, we define the irradiation temperature as:

$$T_{\rm irr} = \left(\frac{F_{\rm irr}}{\sigma}\right)^{1/4} \,. \tag{9}$$

In this paper, the surface optical depth, $\tau_{\rm ex}$, is assumed to be ~ 0.01. This procedure is based on the assumption that the X-ray radiation, caused by the mass accretion upon the compact star, is thermalized *above* the disk surface (at $\tau = 0.01$). This assumption may be justified if the spectrum of the incident X-ray flux is relatively soft (see discussion).

Further, when the semithickness of the disk, Z', is given, the external pressure, $P_{\rm ex}$, is found by solving

$$P_{\rm ex} = \frac{GM}{r^3} Z' \frac{\tau_{\rm ex}}{\kappa(P_{\rm ex}, T_{\rm ex})} \,. \tag{10}$$

© American Astronomical Society • Provided by the NASA Astrophysics Data System

1990ApJ...359..164T

Using the surface boundary conditions (8) and (10), equations (1)–(3) and (7) are integrated from the surface ($z = Z'$ and $\tau = \tau_{ex}$) to the center ($z = 0$). The boundary condition at the center is

$$F_z = 0; \tag{11}$$

however, this condition is not always satisfied for arbitrary pairs of Z' and T_{ex}. We thus iterate the calculations until we find an appropriate Z' for a given T_{ex}, for which the inner boundary condition (11) is fulfilled. By changing values of T_{ex}, we get sequences of solutions which will determine the shape of the thermal equilibrium curves in the (Σ, T) plane. Here the total surface density is $\Sigma \equiv 2\int_0^{Z'} \rho\, dz$, and T is either of $T_c \equiv T(z = 0)$ or $T_{\rm eff} \equiv T(\tau = \frac{2}{3})$. The height of the disk, Z, is defined as the height where $\tau = \frac{2}{3}$.

III. VERTICAL STRUCTURE OF AN IRRADIATED DISK

a) *Thermal Equilibrium Curves*

First we present the thermal equilibrium curves in the (log Σ, log $T_{\rm eff}$) plane at log r (cm) = 10.5 for different irradiation temperatures: $T_{\rm irr} = 0$, 3000, 4500, 6000, 7500, 9000, 10,500, and 12,000 K. The unheated disk, i.e., the disk with $T_{\rm irr} = 0$, has the familiar S-shaped equilibrium curve (Hōshi 1979; Meyer and Meyer-Hofmeister 1981), where the middle branch, with the negative slope, is known to be thermally unstable (see, e.g., Mineshige and Osaki 1983). For those cases in which the mass input rate falls in the thermally unstable region, a steady state is not possible. When the disk is in the lower branch, the surface density will increase due to the low efficiency of the angular momentum transport. Eventually, as the disk reaches the lower turning point, a stable solution ceases to exist and a thermal instability thus sets in and the disk jumps to the high temperature branch on a thermal time scale (Mineshige 1988). Then the high efficiency of the angular momentum transport causes a decrease in the surface density. When the disk reaches the upper turning point, a thermal instability occurs again, and the downward transition is triggered. Hence the disk alternates in this way between the lower and upper branches.

The effect of irradiation upon the S-shaped solution curves, as shown in Figure 1, is substantial. First, the width in surface density of the thermally unstable middle branch, where a triple solution exists, is drastically decreased with the increase of $T_{\rm irr}$. Starting with a range of about 0.3 in log Σ for an unheated disk, it drops to about 0.1 for $T_{\rm irr} = 7500$ K. The unstable portion eventually completely disappears as $T_{\rm irr}$ reaches a certain critical value. This value is found, according to our calculations, to be $T_{\rm irr} \sim 10{,}000$ K. This critical temperature is a weak function of radius, since the effective temperatures of the turning points are less sensitive to radii (see, e.g., FLP; Mineshige and Osaki 1983). Meyer and Meyer-Hofmeister (1984*b*) have indeed noted that strong irradiation can stabilize the disk (see also Saito 1989). An explanation for this behavior using an analytic one zone approximation is presented in § IV. The location of the kink is also effected by the external irradiation. As $T_{\rm irr}$ increases, the upper kink, initially located at log $T_{\rm eff} \sim 3.84$ and log $\Sigma \sim 2.3$, moves to higher effective temperatures and lower surface densities.

The major effect of the external irradiation heating, beyond the modification in the size and location of the unstable kink, takes place on the lower branch of the equilibrium curve. With increasing $T_{\rm irr}$, this part of the curve moves to higher effective temperatures ($T_{\rm eff} \sim T_{\rm irr}$) and becomes almost parallel to the surface density axis. This behavior can clearly be understood in the following way:

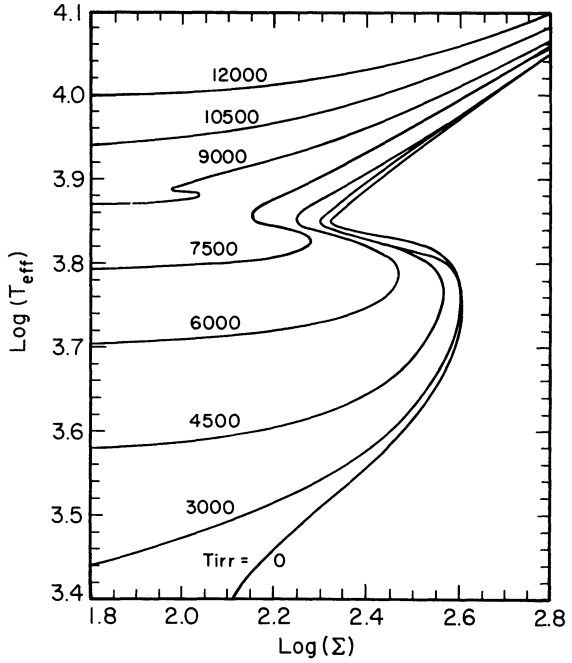

FIG. 1.—Thermal equilibrium curves in the (log $T_{\rm eff}$, log Σ) plane for different irradiation temperatures: $T_{\rm irr} = 0$, 3000, 4500, 6000, 7500, 9000, 10,500, and 12,000 K. The radius is log r (cm) = 10.5, and the viscosity parameter α is taken to be $\alpha = 0.1$.

Integrating equation (3) from the midpoint of the disk to its surface, one gets:

$$F_{ex} = \tfrac{3}{4} W\Omega\,, \tag{12}$$

where W is the integrated viscous stress: $W \equiv 2\int_0^{Z'} \alpha P\, dz$. This relation actually represents the thermal balance in the disk, where the total energy created by the viscous heating is completely emitted by the external net flux. Introducing F_{ex} from equation (8), we get:

$$T_{ex}^{\,4} = \frac{3}{8} f_2(\tau_{ex}) T_{\rm irr}^{\,4} + \frac{3 f_2}{8\sigma}\frac{3}{4} W\Omega\,. \tag{13}$$

Since the energy generation throughout the disk (second term on the right-hand side of eq. [13]) is always positive, one gets the following inequality:

$$T_{\rm eff} > T_{ex} > [\tfrac{3}{8} f_2(\tau_{ex})]^{1/4} T_{\rm irr} \sim 0.9 T_{\rm irr}\,, \tag{14}$$

where we have introduced $\tau_{ex} = 0.01$ into the correction function $f_2(\tau)$ (see Appendix). Thus, $T_{\rm eff}$ cannot be much below $T_{\rm irr}$. The lower branch is thereby increased to higher temperature in the (log Σ, log $T_{\rm eff}$) plane for models with irradiation. Note that because of the partial absorption of the irradiation flux in the photosphere ($Z' > z > Z$ or $\tau < \frac{2}{3}$), $T_{\rm eff}$ is somewhat smaller than $T_{\rm irr}$ in the low-surface density regions; e.g., for $T_{\rm irr} =$ 12,000 K (log $T_{\rm irr} = 4.08$), we find log $T_{\rm eff} \sim 4.0$ at log $\Sigma = 1.8$.

To sum up, the thermal equilibrium curves are rather sensitive to irradiation: for $T_{\rm irr} > 10{,}000$ K, the disk is completely stabilised and no unstable branch is seen, while for $T_{\rm irr} <$ 10,000 K the basic S-shaped equilibrium curves are maintained. The size of the unstable branch, however, is significantly reduced. The value of $T_{\rm eff}$ on the lower branch increases

© American Astronomical Society • Provided by the NASA Astrophysics Data System

1990ApJ...359..164T

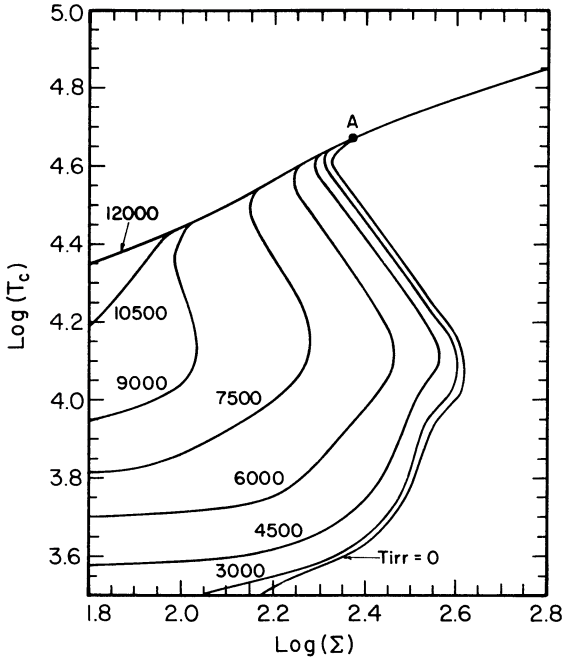

FIG. 2.—Thermal equilibrium curves in the (log T_c, log Σ) plane at log r (cm) = 10.5 for various T_{irr}.

to $\sim T_{irr}$ and the critical surface density, at the upper turning point, decreases. This behavior does not necessarily mean that irradiation modifies the whole vertical structure of the disk.

Since the evolution of the disk is mainly determined by its internal structure, it is useful to present the thermal equilibrium curves also in the (log T_c, log Σ) plane (Fig. 2). At first glance, Figure 2 looks similar to Figure 1, but there are some qualitatively important differences. First, the upper branch is less sensitive to irradiation. As a matter of fact, *all* the equilibrium lines of different irradiation temperatures merge into *one straight* line in the (log Σ, log T_c) plane. As the irradiation temperature increases, however, the surface density at the turning point between the upper and the middle branch decreases. Second, the lower branch is rather sensitive to the irradiation temperature, but not in the same way as in the previous case of effective temperature. The lower branch shows a parallel shift to lower surface densities, keeping the lower turning point almost at the same temperature, rather than giving an overall increase of the lower branch to higher ($\sim T_{irr}$) temperatures. As a consequence, even for $T_{irr} \sim 6000$ K we still see large central temperature differences between the lower and the upper branches.

Figure 3 depicts the relation between T_c and T_{eff}. The dashed line represents the isothermal line, $T_c = T_{eff}$. The plateau in the line of $T_{irr} \sim 0$ at log $T_{eff} \sim 3.8$ is due to an extended partial ionization zone, in which the pressure gradient is mainly supplied by the increase in the number of particles rather than by the increase in temperature. This behavior is also partly supported by the substantial decrease in the opacities of the (vertically) outer region of the disk. Convection is obviously very efficient in this region. When irradiation is present, the outer layers are heated up to T_{irr} independently of T_c, thus lines become, at this stage, parallel to the convective branch of the noninrradiated disk.

b) Vertical Temperature Structure of an Irradiated Disk

In Figures 4 and 5 we illustrate, for a fixed surface density log $\Sigma = 2.45$, the changes in the temperature distributions through the vertical direction of the disk, as caused by different irradiation temperatures for models on the upper and the lower branches, respectively. The substantial difference between the two figures is the direct cause for the behavior of the equilibrium lines in the (log Σ, log T_c) plane (Fig. 2) and in the (log T_{eff}, log T_c) plane (Fig. 3). Note that for log $\Sigma = 2.45$, the lower equilibrium state is present only when $T_{irr} < 5000$ K (Fig. 1).

The equilibrium configurations on the upper branch are completely radiative. According to Figure 4, the modifications due to the external irradiation heating are only appreciable in the extreme surface layer; the main bulk of the mass of the disk remains unaffected. We may therefore conclude that for the upper branch models:

$$T_c \approx T_c^0 , \tag{15}$$

for all irradiation temperatures, where T_c^0 is the central temperature for an unheated disk with the same surface density.

For the lower branch, on the other hand, as a result of efficient convection and relatively small opacities in the outer layers, the effect of irradiation penetrates all the way through the disk (Fig. 5). The increase of temperature due to irradiation, ΔT, is even higher in the central plane than at the surface. Roughly, one gets $\Delta T/T \sim$ const, or

$$T_c = T_c^0\left(1 + \frac{T_{irr} - T_{eff}^0}{T_{eff}^0}\right), \tag{16}$$

where T_{eff}^0 is the effective temperature of the unheated disk, and where we assumed $T_{eff} \simeq T_{irr}$.

Lyutyi and Sunyaev (1976) have suggested the following relation pertains to a radiative disk:

$$T_c^4 = T_{irr}^4 + (T_{eff}^0)^4(1 + \tfrac{3}{4}\tau) , \tag{17}$$

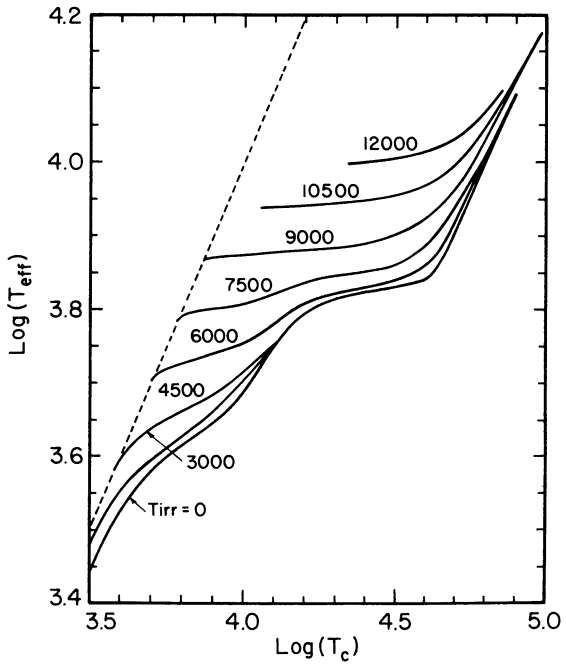

FIG. 3.—Thermal equilibrium curves in the (log T_{eff}, log T_c) plane

© American Astronomical Society • Provided by the NASA Astrophysics Data System

1990ApJ...359..164T

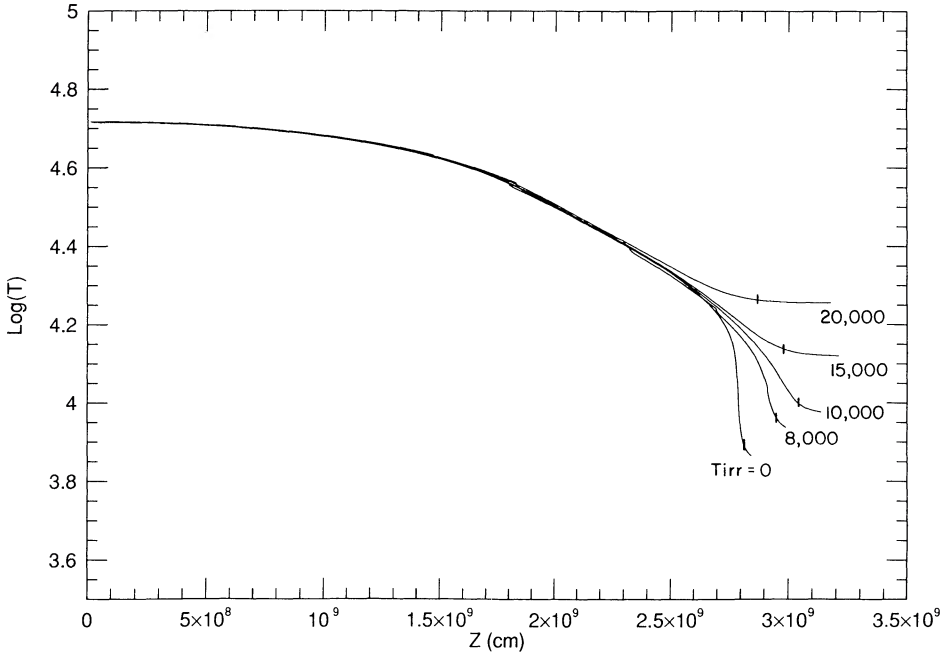

FIG. 4.—Vertical temperature distribution of irradiated accretion disks in the upper radiative branch. The irradiation temperatures and the heights of the photosphere ($\tau = \frac{2}{3}$) are indicated. The surface density is fixed to be log $\Sigma = 2.45$.

where τ is the optical thickness in the vertical direction of the disk, or equivalently:

$$T_c = T_c^0\left[1 + \left(\frac{T_{\rm irr}}{T_c^0}\right)^4\right]^{1/4}. \quad (18)$$

For the upper branch, when $T_{\rm irr} \ll T_c$, equation (18) trivially coincides with equation (15); however, for lower branch disks, the difference between equations (18) and (16) is considerable. For example, assuming a case with a high irradiation temperature for which $T_{\rm irr} \sim T_c^0$, one roughly gets: $T_{\rm eff} \sim T_{\rm irr} \sim T_c^0 \sim 2T_{\rm eff}^0$, where the last similarity is a typical relation for lower branch nonirradiated disks. In this case, equation (18) gives $T_c \sim 1.2T_c^0$, while according to equation (16), $T_c \sim 2T_c^0$. Thus equation (18) is inaccurate for convective disks.

Point A in Figure 2 is defined to be where an unheated disk structure joins the locus of high-temperature solutions of models with various values of $T_{\rm irr}$. For an unheated disk, this point is on the edge of the unstable branch, i.e., near the upper turning point, while for the irradiated disks it is still far from

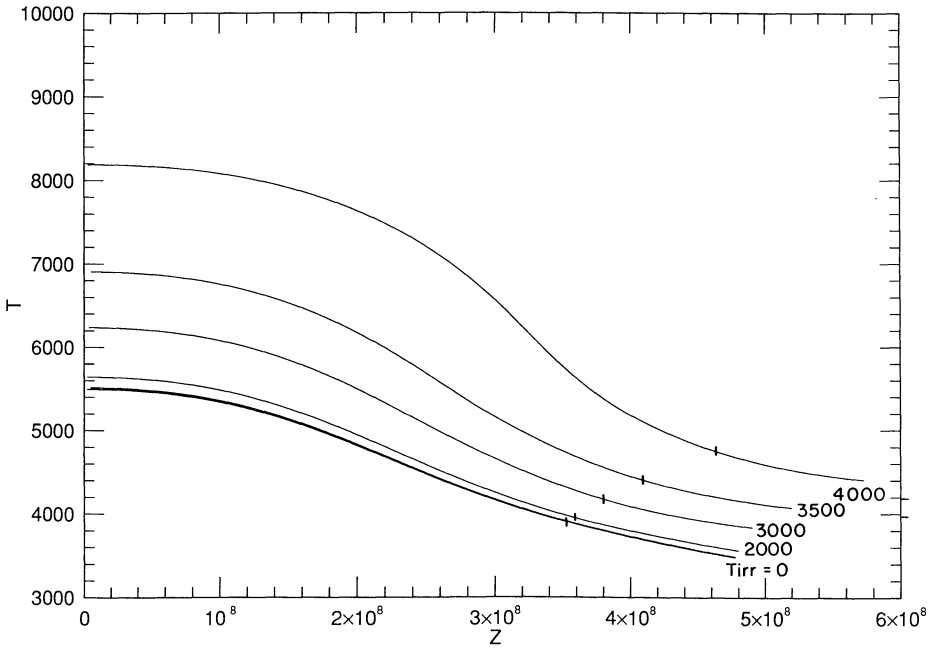

FIG. 5.—Same as Fig. 4, but in the lower convective branch

© American Astronomical Society • Provided by the NASA Astrophysics Data System

1990ApJ...359..164T

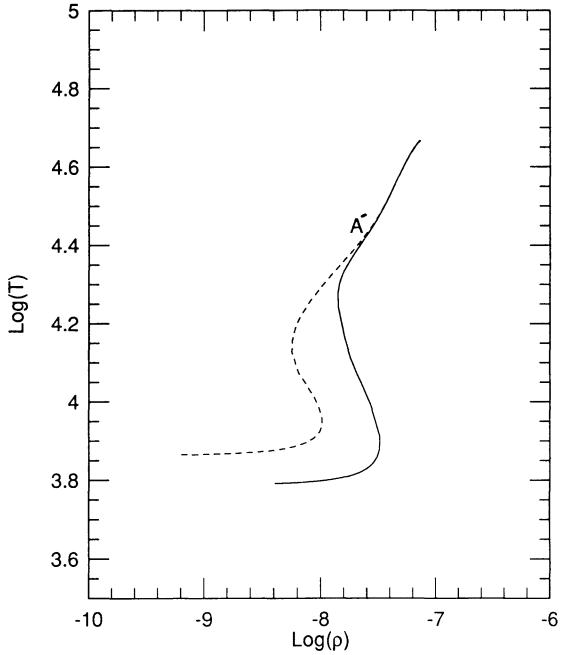

FIG. 6.—Comparison of the vertical structure of the nonirradiated accretion disk (*solid line*) and of the irradiated disk with $T_{irr} = 7500$ K (*dashed lines*) in the (log ρ, log T) plane.

that unstable situation. In Figure 6 we present the detailed structure, in the density-temperature plane, of two models at point A in Figure 2: one (*full line*) without irradiation and the other (*dashed line*) with $T_{irr} = 7500$ K. Figure 6 shows that these two models follow the same path from the center to the height very close to the surface (more than 95% of the disk mass is contained from the center to the point A′ in Fig. 6). The structural profiles in Figure 6 diverge only in the outermost regions. In spite of this extensive similarity, a small decrease in the central temperature of the nonirradiated disk will shift it into a thermally unstable condition, while for the irradiated case, with $T_{irr} = 7500$ K, a decrease of at least 10,000 K is required in order to reach the same situation (see Fig. 2). This fact actually means that the vertical structure is not uniquely determined by the values of the thermodynamical variables at the disk mid-plane, but also by the values of these variables in the outer region. This conclusion will be used and clarified in the next section.

c) *Semithickness of the Disk*

Finally we comment on the changes in the semithickness of the disk induced by the existence of the irradiation. In Figures 4 and 5, the height of the photosphere ($\tau = \frac{2}{3}$) is also indicated by tick marks on each line. In the convective branch (Fig. 5), the disk expands systematically with increasing T_{irr}, because the scale height of the disk at the surface increases with the increasing irradiation temperature. On the other hand, on the radiative branch (Fig. 4), the disk first thickens with increasing irradiation, but for $T_{irr} > 10{,}000$ K, the disk shrinks with increase of T_{irr}. This is caused by the change in the temperature dependence of the opacity (the opacity has a peak at log $T \sim 4.1$). The strong irradiation heats up the gas on the surface and thus forms a tenuous corona-like region above the photosphere of the disk. In these figures, we keep the total surface density constant; but if we allow the gas in the surface layer to escape by obtaining sufficient kinetic energy from the irradiation, then the surface density and hence the total optical depth decrease, leading to the formation of an optically thin disk (Inoue and Hōshi 1987).

IV. SIMPLIFIED ANALYTIC MODEL

a) *Basic Considerations*

The peculiar behavior of the equilibrium solution lines (the S shape) presented in Figures 1–3 and the effect of external irradiation can be clearly understood using a simplified analytic approximation for the vertical structure of disks. Such an approximation has already been used in previous publications (e.g., FLP), however, some modifications of the conventional treatment will supply us with an easy qualitative and quantitative explanation for the existence and the location of the unstable kink, and for the effects of irradiation upon this general behavior of the equilibrium solution lines.

To do so, we first check the importance of the convective energy transport in the thermal equilibrium structures. In Figure 7 we compare the loci of equilibrium solutions with (*solid*) and without (*dashed*) convective energy transport in (log T_c, log Σ) and (log T_{eff}, log Σ) planes. Contrary to the results presented by FLP, the difference between the respective loci is not small, probably because of different adopted values of α ($\alpha = 1.0$ in FLP, while $\alpha = 0.1$ in Fig. 7). Obviously the larger α is, the smaller Σ is, thus the less efficient the convective energy transport becomes (see Cannizzo and Wheeler 1984). The importance of the convection also depends on the radius of the disk, because the equilibrium surface density increases as the radius increases. In fact, Clarke (1987) found a significant contribution by convection in a quasar disk (corresponding to larger radii), while Mineshige and Wheeler (1989) show that in the inner portions of accretion disks in low-mass X-ray binaries convection is very inefficient. The values of Σ or T_{eff} at

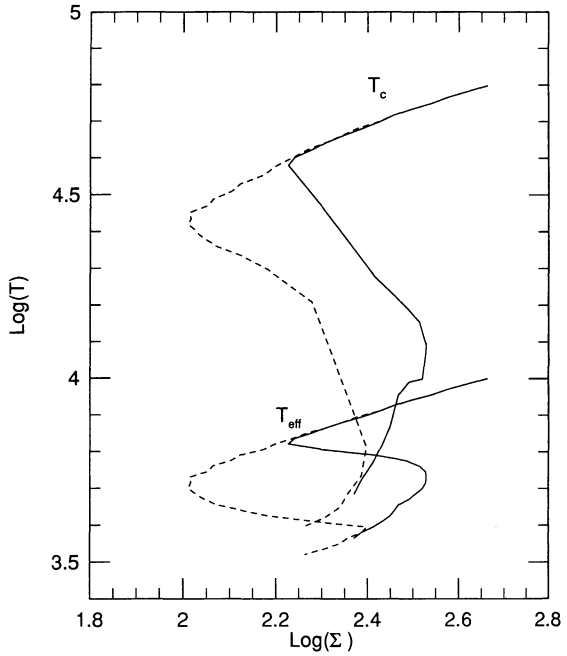

FIG. 7.—Comparison of the thermal equilibrium curves of the model with convective energy transport (*solid lines*) and of the model without convective energy transport (*dashed lines*) in the (log T_{eff}, log Σ) plane (*upper curves*), and in the (log T_c, log Σ) plane (*lower curves*), respectively.

© American Astronomical Society • Provided by the NASA Astrophysics Data System

1990ApJ...359..164T

the turning points are different between the purely radiative model and the convective model; however, the general behavior of these loci, such as the existence of three distinct branches and their slopes, is common to these models. For the sake of simplicity, we shall assume radiation to be the only mode of energy transport through the disk in this section.

Our analysis is based on the assumption that the disk is roughly composed of two regions: the main bulk (or the central zone), which contains most of the mass and where the energy is being produced, and a surface layer (or a transfer zone), which carries the energy from the central region to the surface and out of the disk.

The central zone is relatively homogeneous; thus its structure can be represented by the midplane values of the thermodynamical variables; ρ_c, T_c, and κ_c, standing for the central density, temperature, and opacity, respectively. In the transfer zone, on the other hand, temperatures are decreasing from T_c at the boundary between the central zone to $T_{\rm eff}$ at the surface. The flux in this region is approximately constant and equal to the emergent flux from the disk surface ($=\sigma T_{\rm eff}^4$).

With this simple structure in mind, one can obtain the following relation for a steady unheated disk:

$$\Sigma T_c \propto T_{\rm eff}^4 , \tag{19}$$

which is obtained by integrating equation (3) over the central zone. This relation simply represents the balance between the rates of the viscous energy production in the disk and the energy emitted from it. For the central density, we will use the conventional relation:

$$\rho_c \simeq \frac{\Sigma}{2Z_c} \propto \Sigma T_c^{-1/2} , \tag{20}$$

where Z_c (the depth of the central zone $\sim Z$) is assumed to be proportional to the vertical pressure scale height ($\propto T_c^{1/2}$).

The radiative flux through the transfer zone ($\sim \sigma T_{\rm eff}^4$) can be approximated using equation (4) as:

$$F_{\rm ex} \simeq F_r \propto \frac{T_{\rm ce}^3}{\kappa_{\rm ce}} Z \frac{dT}{dP} , \tag{21}$$

or equivalently, assuming

$$Z \frac{dT}{dP} \propto T_c^{1/2} \frac{T_c}{P_c} \propto \frac{T_c}{\Sigma} , \tag{22}$$

one gets:

$$T_{\rm eff}^4 \propto \frac{T_c}{\Sigma} \frac{T_{\rm ce}^3}{\kappa_{\rm ce}} , \tag{23}$$

where the subscript "ce" stands for a mean value between both edges of the transfer zone. Assuming

$$T_{\rm ce} = (T_c\, T_{\rm eff})^{1/2} , \tag{24}$$

and

$$\kappa_{\rm ce} = \kappa(T_{\rm ce}) , \tag{25}$$

one gets:

$$T_{\rm eff}^4 \propto \frac{T_c}{\Sigma} \frac{(T_{\rm eff}\, T_c)^{3/2}}{\kappa(T_{\rm ce})} . \tag{26}$$

By introducing an analytic approximation for $\kappa_{\rm ce}$, equations (19) and (26) will supply us with any desired relation between the variables: T_c, $T_{\rm eff}$, and Σ. These relations are therefore *completely* controlled by the analytic behavior of the relevant opacities. The conventional power-law fits for the opacities according to Cox and Giuli (1968) are:

$$\kappa = 1.5 \times 10^{20} \rho T^{-5/2} , \tag{27}$$

for the "hot" region, and

$$\kappa = 10^{-40} \rho^{1/3} T^{11} , \tag{28}$$

for the "cold" one. Below 5000 K, *constant* opacities are assumed. The transition temperature, $T_{\rm tr}$, between the "hot" and the "cold" opacities can be obtained by equating expressions (27) and (28). One gets:

$$T_{\rm tr} = 2.87 \times 10^4 ({\rm K}) \rho^{4/81} , \tag{29}$$

e.g., $T_{\rm tr} \simeq (1.15\text{–}1.3) \times 10^4$ K for $\rho = 10^{-8}$ to 10^{-7} g cm^{-3}. Using the general analytic behavior of the opacities presented above, we may roughly identify three regions which will correspond to the three branches found in the curves of equilibrium solutions (Figs. 1–3).

b) *The Upper Branch*

Let us first consider the case of unheated disks. As long as $T_{\rm ce} \geq T_{\rm tr}$, κ is given by equation (27). Substituting equation (27) into equation (26), while assuming $\rho_{\rm ce} \sim \rho_c$ and using equations (19) and (20), one finally gets, after some tedious algebra,

$$\Sigma \propto T_c^{11/4} , \tag{30}$$

or

$$\frac{d \log \Sigma}{d \log T_c} = 2.75 . \tag{31}$$

This relation fits the slope of the upper branch lines in Figure 2 very well. In a similar way, one can also get

$$\Sigma \propto T_{\rm eff}^{44/15} , \tag{32}$$

or

$$\frac{d \log T_{\rm eff}}{d \log \Sigma} = \frac{15}{44} \approx 0.341 , \tag{33}$$

which again fits very accurately the corresponding slope for the nonirradiated case in Figure 1.

Next we discuss the cases of irradiated disks. In § III we have shown that for upper branch equilibrium solutions the penetration of irradiation is limited to the very outer surface layers, thus relations (30) and (31) hold for irradiated disks as well. Equation (19), on the other hand, should be replaced by:

$$\Sigma T_c \propto (T_{\rm eff}^4 - T_{\rm irr}^4) , \tag{34}$$

for the irradiated case. Using equation (30), one gets:

$$\Sigma \propto T_{\rm eff}^{44/15} \left[1 - \left(\frac{T_{\rm irr}}{T_{\rm eff}} \right)^4 \right]^{11/15} . \tag{35}$$

Comparing equation (35) with equation (32), the following conclusion can be drawn: for any given value of the surface density, the equilibrium effective temperature becomes *higher* with the relative increase of irradiation temperature. The shift is determined by the expression in brackets of equation (35). This effect is graphically presented in Figure 1.

© American Astronomical Society • Provided by the NASA Astrophysics Data System

1990ApJ...359..164T

c) Upper Kink

The switch in the slope of the equilibrium solution lines (Figs. 1 and 2) occurs simultaneously with the change of the behavior of the opacity (neglecting convection). This takes place (eq. [29]) as T_{ce} (not T_c) decreases below $T_{tr} \sim 12{,}000$ K (assuming the relevant density range). The transition to the negative slope of the unstable branch will therefore occur when:

$$\log T_{ce} = 0.5(\log T_{eff} + \log T_c) \approx 4.1 . \quad (36)$$

From equations (30) and (32), one easily gets:

$$T_c \propto T_{eff}^{16/15} . \quad (37)$$

This relation indeed fits the behavior of the upper branch disks according to the detailed calculations presented in Figure 3. Using Figure 3 for evaluating the proportionality constant:

$$\log T_c = \tfrac{16}{15} \log T_{eff} + 0.51 . \quad (38)$$

Substituting this expression for the central temperature into equation (36), the effective and the central temperatures of the disk at the upper turning point, T_{eff}^{up} and T_c^{up}, respectively, are thus given by:

$$\log T_{eff}^{up} \approx 3.72 , \quad \log T_c^{up} \approx 4.48 . \quad (39)$$

These values are quite close to the exact ones for a nonconvective disk (Fig. 7, dashed line).

In the case of external irradiation, equation (38) should be replaced by:

$$\log T_c \simeq \frac{16}{15} \log T_{eff} + \frac{4}{15} \log \left[1 - \left(\frac{T_{irr}}{T_{eff}} \right)^4 \right] + 0.51 . \quad (40)$$

Substituting this expression in equation (36), the effective temperature at the upper turning point is now given implicitly by:

$$\log T_{eff}^{up} + \frac{4}{31} \log \left[1 - \left(\frac{T_{irr}}{T_{eff}^{up}} \right)^4 \right] \approx 3.72 . \quad (41)$$

Since the expression in square brackets is smaller than one and approaches zero as T_{irr} increases, T_{eff}^{up} increases with an increase of irradiation temperature, while T_c^{up} decreases with T_{irr} by equation (36). These trends are clearly demonstrated in Figures 1 and 2. As a specific example; for $T_{irr} = 7500$ K, the numerical solution of equation (41) gives $T_{eff}^{up} = 7620$ K which means, using equation (36):

$$\log T_{eff}^{up} \approx 3.88 , \quad \log T_c^{up} \approx 4.32 . \quad (42)$$

These values obviously do not fit those presented in Figures 1 and 2, since they have been reached under the assumption of a radiative disk; however, the effect of irradiation to increase (decrease) T_{eff}^{up} (T_c^{up}) by the amount of $\Delta \log T \sim 0.16$ (compare eqs. [39] and [42]) fits nicely the exact numerical calculations as well (see Figs. 1 and 2).

d) The Middle Unstable Branch

The unstable branch is characterized by a *negative* slope of the equilibrium solution curves. This feature is caused by a corresponding inversion of slope of the opacity (κ_{ce}) as a function of temperature. The power-law approximation for κ_{ce} during this phase is dictated by equation (28) instead of equation (27). Introducing this analytic approximation for the opacity into equation (26) and using equations (19) and (20) to substitute for the effective temperature and the central density (assuming again that $\rho_{ce} \sim \rho_c$), one gets:

$$\Sigma \propto T_c^{-29/20} . \quad (43)$$

This relation gives an excellent fit to the equilibrium curves (Fig. 7, dashed line). Nevertheless, the expression for T_{eff} obtained by equations (19) and (43);

$$\Sigma \propto T_{ef}^{116/9} , \quad (44)$$

does not have even the right sign! This would imply that something is missing in the commonly used relation (19). Indeed, this relation should contain an additional dependence upon the mean molecular weight, μ, which is constant along the upper branch but changes rapidly from 0.5 to 1.0 while crossing the middle branch; namely,

$$\frac{1}{\mu} \Sigma T_c \propto T_{eff}^4 . \quad (45)$$

In the partial ionization zone, μ has a relatively strong (a power of ~ -0.8) dependence upon the central temperature. Introducing this dependance into equation (45) and using relation (44), we get:

$$\Sigma \propto T_{eff}^{-116/7} . \quad (46)$$

which fits the calculated data much better (Fig. 7, T_{eff} dashed line).

e) The Lower Branch

The termination of the middle branch occurs as soon as κ_{ce} ceases to behave according to equation (28), namely, as T_{ce} drops below ~ 5000 K. Indeed, using Figure 7 to determine the temperatures at the lower turning point of the kink, one finds:

$$\log T_{eff}^{lw} \approx 3.6 , \quad \log T_c^{lw} \approx 3.8 . \quad (47)$$

Using these values in equation (35), one gets: $\log T_{ce}^{lw} \approx 3.7$ and thus $T_{ce}^{lw} \sim 5010$ K, fitting precisely our previous expectations.

In the lower branch, we may assume κ_{ce} to be constant. Thus, according to equations (19) and (26), one gets:

$$\Sigma \propto T_c^{15/13} , \quad (48)$$

and

$$\Sigma \propto T_{eff}^{15/7} . \quad (49)$$

Note that in the presence of the external irradiation, the slope of this branch becomes flatter than in the nonirradiated situations, as is seen in Figures 1 and 2.

V. DISCUSSION AND CONCLUSIONS

a) Thermalization of External Heat Sources

In this paper, we assumed that the external flux from the central portions of the accretion disk and from the central object is thermalized in the surface layer. In general, X-ray spectra of low-mass X-ray sources are relatively soft (mostly $E \leq 10$ keV). In contrast, in massive X-ray binaries, black hole binaries (e.g., Cyg X-1), or active galactic nuclei, the hard X-ray tail extends to 200 keV, or even to the gamma-ray range. Our assumption of surface thermalization may not be justified if the hard component of the radiation is strong and irradiation deeply penetrates the disk. Our present results suggest that conditions might have to be fairly extreme before our current models are severely modified. The radiative portions of the disk structure are difficult to perturb, and this should remain

© American Astronomical Society • Provided by the NASA Astrophysics Data System

1990ApJ...359..164T

true even if heating occurs beneath the photosphere as long as heating is confined to a reasonably small outer region. For the convective portions of the structure, the entire vertical structure is already subject to heating by the rapid convective mixing, so the precise distribution of the additional heat source may not be a major effect. These tentative conclusions need to be checked for both radiative and convective structure to determine the effects of distributing the external heating throughout the vertical structure.

If the energy spectrum of the irradiation is in the hard X-ray range, then the situation might also be different for another reason. As Begelman, McKee, and Shields (1983) proposed, a Compton-heated wind is a more plausible consequence in that case. Portions of the mass in the disk might escape from the disk (Inoue and Hōshi 1987; Hōshi and Inoue 1988), leading to overstable oscillations in the mass flow through the disk (Shields *et al.* 1986). The calculations of such a case need a full treatment of radiative transfer, however, and so they are beyond the scope of this paper. Our treatment is only fully justified when the spectrum of the irradiation flux is relatively soft.

b) Basic Considerations for Observational Implications

Shakura and Sunyaev (1973) gave a simple formula to evaluate the irradiation flux, $F_{\rm irr}$; that is,

$$F_{\rm irr} = C\,\frac{L_X}{2\pi r^2}\,. \tag{50}$$

Here we have assumed that the irradiation flux is proportional to the X-ray luminosity, L_X, and C is a parameter representing the fraction of the X-ray energy which is caught by the outer disk.

It is not easy to get a reasonable estimate for C from theoretical considerations, because it depends critically on the geometry and the emission mechanism of the soft and hard X-rays. Shakura and Sunyaev (1973) presented the following estimates;

$$C \sim \begin{cases} A\,\dfrac{d}{d\ln r}\left(\dfrac{H}{r}\right) & \text{for a neutron star binary;} \\ A\,\dfrac{d}{d\ln r}\left(\dfrac{H}{r}\right)^2 & \text{for a black hole binary,} \end{cases} \tag{51}$$

where A is the X-ray albedo. The difference in equations (51) come from different geometries of the emitting regions. Shakura and Sunyaev (1973) assume that in a neutron star binary the X-rays are radiated from a neutron star surface more or less isotropically, whereas in a black hole binary the X-ray flux comes from the inner portions of the disk and is therefore radiated predominantly in the direction vertical to the disk plane. From the relation of hydrostatic balance,

$$\frac{H}{r} \sim 0.02\left(\frac{T}{10^4}\right)^{1/2}\left(\frac{M}{M_\odot}\right)^{-1/2}\left(\frac{r}{10^{10.5}}\right)^{1/2}, \tag{52}$$

where C is numerically estimated with equation (51) to be between $C \sim 10^{-2}$ (neutron star of $M = 1\ M_\odot$) and 10^{-5} (black hole of $10\ M_\odot$) for $A \sim 1$.

The above estimates are based on the assumption that X-ray emission is not shielded by the inner portions of the disk. It has been demonstrated, however, that in a steady convective accretion disk model the outer convective regions are shaded from direct irradiation (Meyer and Meyer-Hofmeister 1982); the standard-disk relation, $H/r \propto r^{9/8}$ (Shakura and Sunyaev 1973), is no longer correct because of the convection. In the following, we thus do not specify the value of C, but instead discuss what values are required for C if the light variations of the disk are caused by the dwarf nova–type thermal instability.

Leaving the value of C as a free parameter, the irradiation temperature is numerically expressed in terms of the X-ray luminosity as

$$T_{\rm irr} \simeq 10^{3.9}\,({\rm K})\left(\frac{C}{10^{-4}}\right)^{1/4}\left(\frac{L_X}{10^{37}}\right)^{1/4}\left(\frac{r}{10^{10.5}}\right)^{-1/2}. \tag{53}$$

With the steady state assumption, the mass accretion rate, $\dot{M}_a$, is equal to the mass transfer rate (or mass input rate), $\dot{M}_0$. Then L_X is approximately

$$L_X = \frac{GM\dot{M}_0}{R_{\rm in}}\,. \tag{54}$$

Inserting equation (53) into equation (51), we finally get

$$T_{\rm irr} \simeq 10^{3.9}\,({\rm K})\left(\frac{C}{10^{-4}}\right)^{1/4}\left(\frac{\dot{M}_0}{10^{17}}\right)^{1/4}\left(\frac{r}{10^{10.5}}\right)^{-1/2} \times \left(\frac{R_{\rm in}}{10^6}\right)^{-1/4}\left(\frac{M}{M_\odot}\right)^{-1/4}. \tag{55}$$

When the disk is entirely in the hot radiative state, then the shielding of the X-ray flux by the inner portions of disk is inefficient, and C is more likely to be of order $H/r \sim 10^{-2}$. From equation (55), we have $T_{\rm irr} \simeq 10^{4.4}\ {\rm K} > T_{\rm crit} = 10^4\ {\rm K}$ for typical values of $\dot{M}_0$, r, $R_{\rm in}$, and M (shown in eq. [55]). With such strong irradiation, the disk is thus stabilized against the thermal instability. On the other hand, in the decay phase or quiescence, when the outer regions of the disk are in the cool state, the X-rays cannot reach the outer portions of the disk directly; thus C should be extremely small. For $C \sim 10^{-5}$, we get $T_{\rm irr} \sim 10^{3.7} < T_{\rm crit}$ at $r = 10^{10.5}$ cm.

This means that a disk artificially maintained in the hot radiative state by irradiation is in a precarious condition. Any fluctuation which led to a swelling at intermediate radii which thus shielded the outer portions would allow the outer edge of the disk to precipitately enter a cooling phase.

Meyer and Meyer-Hofmeister (1984*b*) considered indirect irradiation which reaches the disk by X-ray light scattered at the surface of the secondary and by the light scattered in a hot corona, and estimate the values of $T_{\rm irr}$ appropriate for Her X-1 ($M = 1.33\ M_\odot$, $r_R = 10^6$ cm, and $\dot{M}_0 = 10^{17.3}$ g s^{-1}) in three ways:

$$T_{\rm irr} \sim 6000\ ({\rm K})\,, \tag{56a}$$

$$T_{\rm irr} = 10^{3.3}\ ({\rm K})\left(\frac{r}{10^{11}}\right)^{-5/6}, \tag{56b}$$

$$T_{\rm irr} = 10^{3.7}\ ({\rm K})\ \beta^{1/7}\left(\frac{r}{10^{11}}\right)^{-11/14}. \tag{56c}$$

Here $\beta(\geq 1/25)$ is the fraction of the irradiation energy dissipated in the corona. Note their estimates correspond to $C \sim 10^{-5}$ to 10^{-4} in equation (55). In contradiction to their conclusion that the dwarf nova–type instability is suppressed in this X-ray binary, their values of $T_{\rm irr}$ indicate that the outer portions of the disk ($r \geq 10^{11}$ cm) are still thermally unstable, because $T_{\rm irr} < 10{,}000$ K there.

© American Astronomical Society • Provided by the NASA Astrophysics Data System

1990ApJ...359..164T

c) Soft X-Ray Transients

The averaged mass-transfer rates of some soft X-ray transients are listed in Table 1 of White, Kaluzienski, and Swank (1984): $\log \dot{M} \sim 14$–15 for A0620−00, Aql X-1, and Cen X-4, while $\log \dot{M} \sim 16.6$–16.8 for 4U1630−47 and 4U1608−52. This implies that the stabilizing effects of the irradiation are stronger for the latter group stars. In fact, their light curves show a plateau in the decay from outburst (White, Kaluzienski, and Swank 1984; Priedhorsky and Holt 1987) presumably caused by irradiation. If the dwarf nova–type disk instability is really responsible for the light variations in 4U1630−47 and 4U1608−52, then C should be as low as $\sim 10^{-4}$ from equation (55).

On the other hand, we can show that even larger values of $C(\sim 10^{-2})$ are not sufficient to suppress the thermal instability in Aql X-1 and Cen X-4 in the low L_X state. Van Paradijs *et al.* (1987) reported that the X-ray luminosity in the low state of these transients is L_X (0.5–4.5 keV) $< 3.0 \times 10^{33}$ ergs s^{-1} for Aql X-1, and L_X (0.5–4.5 keV) $\simeq 1.5$ to 4.2×10^{33} ergs s^{-1} for Cen X-4. From equation (53), we find $T_{\rm irr} \leq 4000$ K, definitely below the critical irradiation temperature of 10,000 K. Here we assumed that most of the radiation is in the soft X-ray range. We may thus conclude that the dwarf nova–type thermal instability is a plausible cause of the transient behavior in Aql X-1 and Cen X-4.

Similarly, outbursts of A0620−00 may be triggered by the thermal instability, because the X-ray luminosity at quiescence is below 10^{32} ergs s^{-1}, corresponding to $T_{\rm irr} \leq 1000$ K even for $C \sim 10^{-2}$. The thermal transitions of the disk A0620−00 are an inevitable consequence. Note, however, the optical light curve of A0620−00 given by Whelan *et al.* (1977) also displays a plateau in the decay (see also the X-ray light curve in Matilsky *et al.* 1976). If this plateau is really caused by the irradiation, C is estimated as $C \sim 10^{-5}$ to 10^{-4} for L_X (max) $\sim 10^{38}$ ergs s^{-1} (eq. [53]). This value is consistent with the value estimated by Meyer and Meyer-Hofmeister (1984*b*). The same conclusion may be derived for the newly discovered X-ray nova GS 2000+25, which is very similar to A0620−00 in many respects (Tsunemi *et al.* 1989).

In the maximum state, the observed L_X is high in Aql X-1, Cen X-4, and A0620−00. At face value, the X-ray flux is sufficient to maintain the hot radiative state. We thus still need a mechanism to initiate the downward thermal transition from the high state to the low state. This may be caused by the wind mass loss from the disk, which reduces $\dot{M}_a$, L_X, and $T_{\rm irr}$ (eq. [55]), or by the shielding of the outer portions of the disk from the X-rays. The irradiated portions of the disk may be in an unstable equilibrium in the sense that an increase in heating will fatten the disk and maintain the high state, but a decrease will shrink the vertical height, leading directly to shielding and hence a cooling instability. The time scales of the perturbations then become a key question. We need time-dependent calculations of irradiated accretion disks.

d) Other X-Ray Binaries

Cannizzo, Wheeler, and Ghosh (1985) pointed out that, although Her X-1 falls on the thermally unstable region in the ($r_{\rm out}$, $\dot{M}_0$) plane, it shows no outburst of the type observed in Cen X-4 and Aql X-1. This is probably because the existence of the magnetosphere causes strong X-ray irradiation by hard X-rays so that the outer portions of the disk are completely stabilized against the dwarf nova–type thermal instability. It is still not completely clear why Cen X-4 and Aql X-1, with similar parameters, are not subject to such strong irradiation and do show outbursts.

In Cyg X-1, the effects of irradiation will be much stronger because of its high mass transfer rate. The steady state model, however, implies that the temperature of the outer portions of the disk at $r = 10^{11}$ cm is below the critical temperature for the dwarf nova–type instability (~ 8000 K):

$$T_{\rm eff} \simeq 4000\,({\rm K})\left(\frac{\dot{M}_0}{10^{17}}\right)^{1/4}\left(\frac{r}{10^{11}}\right)^{-3/4}\left(\frac{M}{10\ M_\odot}\right)^{1/4}. \quad (57)$$

As long as the irradiation flux is weak ($C \leq 10^{-4}$), the disk in Cyg X-1 should undergo the thermal instability. The 300 day periodicity in the soft X-ray component (Priedhorsky, Terrell, and Holt 1983) may be induced by the thermal transitions. Since the secondary star is much brighter than the accretion disk in optical light, optical light variations are not expected, even if the 300 day X-ray variation involves an optical variation with the same periodicity. The reason for the shorter recurrence period (~ 300 days) in Cyg X-1 (versus ~ 60 yr in A0620−00) may be due to the high mass transfer rate and high irradiation (Wheeler *et al.* 1990; Mineshige, Kim, and Wheeler 1990).

e) Galactic Nuclei

Finally, we should note the case of galactic nuclei. The disk thermal instability model may also be relevant to disks in galactic nuclei (Lin and Shields 1986). Such model disks exhibit similar transitions between the hot and the cool states, which may account for the variable energetics of quasars (see Mineshige and Shields 1990, and references therein). The irradiation temperature for AGNs is estimated to be

$$T_{\rm irr} \simeq 10^{3.15}\,({\rm K})\left(\frac{C}{10^{-4}}\right)^{1/4}\left(\frac{L_X}{10^{45}}\right)^{1/4}\left(\frac{r}{10^{16}}\right)^{-1/2}. \quad (58)$$

If the X-ray radiation is isotropic, we find

$$C \sim A\left(\frac{H}{r}\right) \simeq 10^{-3.5}\left(\frac{A}{0.5}\right)\left(\frac{T}{10^4}\right)^{1/2}\left(\frac{M}{10^8\ M_\odot}\right)^{-1/2}\left(\frac{r}{10^{16}}\right)^{1/2}. \quad (59)$$

The luminosity of the steady disk with accretion rate $\dot{M}_0$ is estimated to be

$$L_0 = \epsilon \dot{M}_0 c^2 \sim 10^{45.8}\,({\rm ergs})\left(\frac{\epsilon}{0.1}\right)\left(\frac{\dot{M}_0}{1\ M_\odot\ {\rm yr}^{-1}}\right), \quad (60)$$

and the unstable radius, which is defined as the radius where the effective temperature for the steady model with $\dot{M}_0$ becomes the lower critical temperature (~ 5000 K), is (Mineshige and Shields 1990)

$$r \approx 10^{16.4}\,({\rm cm})\left(\frac{\dot{M}_0}{1\ M_\odot\ {\rm yr}^{-1}}\right)^{0.37}\left(\frac{M}{10^8\ M_\odot}\right)^{-1/2}. \quad (61)$$

Thus $T_{\rm irr} \sim 2000$ K for the steady state with $\dot{M}_0 = 1\ M_\odot$ yr^{-1} and $L = L_0$, and $T_{\rm irr} \sim 5000$ K at maximum light of $L = L_{\rm max} \sim 10^{1.5} L_0$. The effect of irradiation on the thermal instability can be completely neglected in the low state and is of marginal importance in the high state. This situation is quite analogous to the case of A0620−00. The efficient irradiation around the luminosity peak may create a plateau in the decline phase in the light curves of AGNs (similar to A0620−00) and also form a 3 μm bump in the spectra, which could not be

© American Astronomical Society • Provided by the NASA Astrophysics Data System

1990ApJ...359..164T

explained by the nonirradiated disk model (see discussion in Mineshige and Shields 1990, and references therein).

f) Conclusions

1) In radiative disks, irradiation cannot penetrate deeply into the disk, but only heats up the surface layer, which is consistent with the simple analysis by Lyutyi and Sunyaev (1976).

2) In convective disks, the irradiation changes the overall thermal structure of the disk. For a sufficiently strong irradiation, the hydrogen and helium atoms are completely ionized, and thus the thermal instability is suppressed. The critical irradiation temperature is $T_{\rm crit} \sim 10{,}000$ K, where the irradiation flux is given by $F_{\rm crit} = \sigma T_{\rm crit}^4$.

3) In systems with relatively high mass transfer rates (e.g., $\dot{M} \sim 10^{17}$ g s^{-1}), if the shielding effect of the inner portions of the disk is inefficient, the entire disk structure is subject to the X-ray irradiation, and thus the dwarf nova–type thermal instability is suppressed as discussed by Meyer and Meyer-Hofmeister (1984*b*). If the shielding is effective, then we get light variations, but the amplitudes may be reduced (of order 1–2 mag). The 300 day modulation of the soft X-ray luminosity in Cyg X-1 might be caused by the thermal instability.

4) In systems with relatively low mass transfer rates (e.g., $\dot{M} \sim 10^{15}$ g s^{-1}) such as Aql X-1, Cen X-4, and A0620−00, irradiation can be completely neglected in quiescence, the disk is thus unstable against the dwarf nova–type instability. This mechanism may also be relevant to GS 2000+25. At maximum light, however, irradiation may suppress the instability. Then we require a mechanism to initiate the downward thermal transition and speculate that an equilibrium irradiated disk might nevertheless be unstable in some circumstances. Wind mass loss of the disk might help reduce the irradiation flux.

We wish to thank to G. A. Shields, E. Vishniac, and M. Huang for their fruitful discussion and critical comments. S. M. is also grateful to D. E. Baldwin, H. Berk, T. Tajima, and other staffs at the Institute for Fusion Studies for their hospitality. Numerical calculations were performed on the Cray X-MP at the University of Texas System Center for High Performance Computing. This research was supported in part by NSF grant 8717166, NASA grant NSG 7232, and US Department of Energy DE-FG05-80 ET53088.

APPENDIX

DISCRETE ORDINATE APPROXIMATION OF FOURTH ORDER

This is an extension of the Eddington approximation (discrete ordinate approximation of second order) including higher order corrections. The correction factors $f_1(\tau)$ and $f_2(\tau)$ are written as

$$f_2(\tau) = \tau + Q - \sum_{n=1}^{4} L_n \exp(-K_n \tau) , \tag{A1}$$

and

$$f_1(\tau) = df_2(\tau)/d\tau . \tag{A2}$$

Here

$$(L_1, L_2, L_3, L_4) = (0.0329, 0.051, 0.0369, 0.0121) , \tag{A3}$$

$$(K_1, K_2, K_3, K_4) = (20.036, 3.7959, 1.6959, 1.1279) , \tag{A4}$$

$$Q = 0.710453 . \tag{A5}$$

In the limits of $\tau \gg 1$ or $\tau = \frac{2}{3}$, we find

$$f_1(\tau) \sim \begin{cases} 1 & \text{for } \tau \gg 1 ; \\ \frac{4}{3} & \text{for } \tau = \frac{2}{3} . \end{cases} \tag{A6}$$

Results of our paper are only slightly changed by replacing $f(2)$ by $(\tau + \frac{2}{3})$ and $f(1)$ by 1, which gives the common Eddington approximation. For details, see chapter 25 in Chandrasekhar (1950).

REFERENCES

Begelman, M. C., McKee, C. F., and Shields, G. A. 1983, *Ap. J.*, **271**, 70.
Cannizzo, J. K., and Wheeler, J. C. 1984, *Ap. J. Suppl.*, **55**, 367.
Cannizzo, J. K., Wheeler, J. C., and Ghosh, P. 1985, in *Proc. Cambridge Workshop on Cataclysmic Variables and Low-Mass X-Ray Binaries*, ed. D. Q. Lamb and J. Patterson (Dordrecht: Reidel), p. 307.
Cannizzo, J. E., Wheeler, J. C., and Polidan, R. S. 1986, *Ap. J.*, **301**, 634.
Chandrasekhar, S. 1950, *Radiative Transfer* (Oxford: Clarendon Press).
Clarke, C. J. 1987, Ph.D. thesis, Oxford University.
Cox, A. N., and Stewart, J. N. 1970, *Ap. J. Suppl.*, **19**, 243.
Cox, J. P., and Guili, R. T. 1968, *Principles of Stellar Structure* (New York: Gordon & Breach), § 14.
Faulkner, J., Lin, D. N. C., and Papaloizou, J. C. B. 1983, *M.N.R.A.S.*, **205**, 359 (FLP).
Hameury, J. M., King, A. R., and Lasota, J. P. 1986, *Astr. Ap.*, **162**, 71.
———. 1987, *Astr. Ap.*, **171**, 140.
———. 1988, *Astr. Ap.*, **192**, 187.
Hayakawa, S. 1981, *Pub. Astr. Soc. Japan*, **33**, 365.
Hōshi, R. 1979, *Progr. Theor. Phys.*, **61**, 1307.
Hōshi, R., and Inoue, H. 1988, *Pub. Astr. Soc. Japan*, **40**, 421.
Huang, M., and Wheeler, J. C. 1989, *Ap. J.*, **343**, 229.
Inoue, H., and Hōshi, R. 1987, *Ap. J.*, **322**, 320.
Lin, D. N. C., Papaloizou, J., and Faulkner, J. 1985, *M.N.R.A.S.*, **212**, 15.
Lin, D. N. C., and Shields, G. A. 1986, *Ap. J.*, **305**, 28.
Long, K. N., Helfand, D. J., and Grabelsky, D. A. 1981, *Ap. J.*, **248**, 925.
Lynden-Bell, D., and Pringle, J. E. 1974, *M.N.R.A.S.*, **168**, 603.
Lyutyi, V. M., and Syunyaev, R. A. 1976, *Soviet Astr.*, **20**, 290.

© American Astronomical Society • Provided by the NASA Astrophysics Data System

1990ApJ...359..164T

Matilsky, T., *et al.* 1976, *Ap. J.* (*Letters*), **210**, L127.
Mayer, F., and Meyer-Hofmeister, E. 1981, *Astr. Ap.*, **104**, L10.
———. 1982, *Astr. Ap.*, **106**, 34.
———. 1984*a*, *Astr. Ap.*, **132**, 143.
———. 1984*b*, *Astr. Ap.*, **140**, L35.
Mineshige, S. 1986, *Pub. Astr. Soc. Japan*, **38**, 831.
———. 1988, *Astr. Ap.*, **190**, 72.
Mineshige, S., Kim, S-W., and Wheeler, J. C. 1990, *Ap. J.* (*Letters*), in press.
Mineshige, S., and Osaki, Y. 1983, *Pub. Astr. Soc. Japan*, **35**, 377.
———. 1985, *Pub. Astr. Soc. Japan*, **37**, 1.
Mineshige, S., and Shields, G. A. 1990, *Ap. J.*, **351**, 47.
Mineshige, S., Tuchman, Y., and Wheeler, J. C. 1990, *Ap. J.*, **359**, 176 (Paper II).
Mineshige, S., and Wheeler, J. C. 1989, *Ap. J.*, **343**, 241.
Osaki, Y. 1974, *Pub. Astr. Soc. Japan*, **26**, 429.
Paczyński, B. 1969, *Acta Astr.*, **19**, 1.
Papaloizou, J., Faulkner, J., and Lin, D. N. C. 1983, *M.N.R.A.S.*, **205**, 487.
Priedhorsky, W. C., and Holt, S. S. 1987, *Space Sci. Rev.*, **45**, 291.
Priedhorsky, W. C., Terrell, J., and Holt, S. S. 1983, *Ap. J.*, **270**, 233.
Pringle, J. E. 1981, *Ann. Rev. Astr. Ap.*, **19**, 137.
Pringle, J. E., Verbunt, F., and Wade, R. A. 1986, *M.N.R.A.S.*, **221**, 169.
Saito, N. 1989, *Pub. Astr. Soc. Japan*, submitted.
Shakura, N. I., and Sunyaev, R. A. 1973, *Astr. Ap.*, **24**, 337.
Shields, G. A., McKee, C. F., Lin, D. N. C., and Begelman, M. C. 1986, *Ap. J.*, **306**, 90.
Smak, J. 1982, *Acta Astr.*, **32**, 199.
———. 1984, *Acta Astr.*, **34**, 161.
Spiegel, E. A. 1963, *Ap. J.*, **138**, 216.
Tsunemi, H., Kitamoto, S., Okamura, S., and Roussel-Dupré, D. 1989, *Ap. J.* (*Letters*), **337**, L81.
Tuchman, Y., Sack, N., and Barkat, Z. 1978, *Ap. J.*, **219**, 183.
van Paradijs, J., and Verbunt, F. 1984, in *High Energy Transients in Astrophysics*, ed. S. E. Woosley (AIP Conf. Proc. No. 115), p. 49.
van Paradijs, J., Verbunt, F., Shafer, R. A., and Arnaud, K. A. 1987, *Astr. Ap.*, **182**, 47.
Wheeler, J. C., Mineshige, S., Huang, M., and Kim, S-W. 1990, in *Proc. 11th North American Workshop on CVs and LMXBs*, ed. C. Mauche (Cambridge: Cambridge University Press), in press.
Whelan, J. A. J., *et al.* 1977, *M.N.R.A.S.*, **180**, 657.
White, N. E., Kaluzienski, J. L., and Swank, J. H. 1984, in *High Energy Transients in Astrophysics*, ed. S. E. Woosley (AIP Conf. Proc. No. 115), p. 31.

S. MINESHIGE: Institute of Astronomy, University of Cambridge, Madingley Road, Cambridge CB3 0HA, UK

T. TUCHMAN: Department of Physics, Hebrew University, Jerusalem, Israel

J. C. WHEELER: Astronomy Department, The University of Texas at Austin, RLM 15.308, Austin TX 78712-1083

© American Astronomical Society • Provided by the NASA Astrophysics Data System

1990ApJ...359..164T

THE ASTROPHYSICAL JOURNAL, 359:176–185, 1990 August 10
© 1990. The American Astronomical Society. All rights reserved. Printed in U.S.A.

STRUCTURE AND EVOLUTION OF IRRADIATED ACCRETION DISKS. II. DYNAMICAL EVOLUTION OF A THERMALLY UNSTABLE TORUS

S. MINESHIGE,[1,2] Y. TUCHMAN,[3] and J. C. WHEELER
Department of Astronomy, University of Texas at Austin
Received 1989 October 11; accepted 1990 January 9

ABSTRACT

The nonlinear evolution of the thermal instability in nonirradiated and irradiated accretion disk annuli is studied using a one-dimensional dynamical code. First we calculate nonirradiated models. It is shown that the thermal instability propagates in the vertical direction, keeping $\delta F_z/F_z$ constant, while $\delta T/T$ is variable, where δ represents the time variation and F_z is the vertical energy flux. The dynamical calculations confirm that the disk-instability model can well account for the UV delay and the presence of a Balmer jump detected in some dwarf-nova outbursts.

Effects of irradiation on the thermal instability of accretion disks are investigated according to the following three cases. In the first case, the irradiation flux is fixed. Moderately strong irradiation with $T_{\rm irr} \sim 6000$ K, where the irradiation flux is defined as $F_{\rm irr} = \sigma T_{\rm irr}^4$, is shown to reduce the amplitude and the quiescent times and to increase the outburst duration of the resultant light curves. Such light curves are observed in some X-ray binaries, including Cyg X-1. In the second case, in which $F_{\rm irr}$ varies in proportion to the mass accretion rate at the inner edge of the disk, $\dot{M}_a$, we succeed in reproducing light curves with a plateau in the decay from outbursts by introducing a time delay in the response of $F_{\rm irr}$ to the modulation in $\dot{M}_a$. Such a light curve is very reminiscent of the light curves of black-hole candidate A0620−00 and of some soft X-ray transients which contain neutron stars. In the third case, in which irradiation is suddenly switched on, it is shown that the surface temperature of the disk rises even faster than the central temperature, leading to a temperature inversion. This would cause wind mass loss and the formation of an accretion corona.

Subject headings: stars: accretion — stars: dwarf novae — X-rays: binaries

I. INTRODUCTION

The theory of accretion-disk thermal instability, which is caused by the partial ionization of hydrogen and helium, was first proposed for outbursts of dwarf novae (Osaki 1974; Hōshi 1979; Meyer and Meyer-Hofmeister 1981) and has been applied to various kinds of astrophysical objects, such as symbiotic stars (Duschl 1986*a*, *b*), soft X-ray transients (Cannizzo, Wheeler, and Ghosh 1985; Huang and Wheeler 1989; Mineshige and Wheeler 1989), and galactic nuclei (Lin and Shields 1986; Clarke 1987; Mineshige and Shields 1990). For relevant mass-transfer rates and masses of central objects, disks are shown to be thermally unstable and thus exhibit time-dependent light variations, similar to observed outburst-quiescent cycles of dwarf novae. It is argued, however, that the dwarf nova–type thermal instability is suppressed by the presence of strong irradiation (Meyer and Meyer-Hofmeister 1984; Saito 1990). The effect of irradiation on the thermal instability is therefore a key factor in the construction of successful models for X-ray binaries and active galactic nuclei.

In Paper I (Tuchman, Mineshige, and Wheeler 1990) we have studied the effects of irradiation on the thermal instability properties of static accretion disk models. It is shown that in the hot state, in which hydrogen and helium are fully ionized, only the surface layer is heated by external irradiation, and so the internal structure is almost unaffected (see also Lyutyi and Syunyaev 1976). On the other hand, in the middle or cool states, in which hydrogen and helium are recombined or only partially ionized, the entire structure is altered by the presence of the irradiation. As a consequence of these properties of the disk, the thermally unstable branch disappears for strong irradiation with $T_{\rm eff} > 10{,}000$ K, where the irradiation flux is $F_{\rm irr} \equiv \sigma T_{\rm eff}^4$; the disk becomes totally thermally stable, and no time-dependent behavior will emerge. In contrast, if the irradiation is not so strong ($T_{\rm eff} < 10{,}000$ K), the thermally unstable branch still remains in the thermal equilibrium curve. We thus expect time-dependent activity associated with the thermal instability, similar to the case of dwarf novae. We estimated the typical strength of irradiation in soft X-ray transients and concluded that the effects of irradiation can be ignored in quiescence, when the X-ray flux is low. We also argued that in the decline phase, the irradiation cannot prevent the propagation of the cooling wave, because the outer cooler portions of the disk are shaded by the inner hot regions.

In the present paper, we focus on the dynamical response of a one-zone torus (or annulus) to the thermal instability and to external heat sources. The detailed methods of the dynamical calculations are described in § II. We use essentially the same methods which are used to calculate stellar models. One major difference is that in the present calculations we allow the mass contained in a torus to change owing to continuous mass input or mass output. Changes in the surface density of the torus are described by the one-zone torus model (Mineshige and Osaki 1983, hereafter MO83).

Results of the dynamical evolution of the thermally unstable torus are presented for the case of no irradiation in § III. All previous time-dependent calculations assumed hydrostatic balance in the vertical direction, because the sound crossing time scale for the vertical direction, $\tau_h \sim \Omega^{-1}$, is shorter than the thermal time scale, $\tau_{\rm th} \sim (\alpha\Omega)^{-1}$, by a factor $\alpha^{-1}(>1)$ in

[1] Also at Institute for Fusion Studies, University of Texas at Austin.
[2] Present address: Institute of Astronomy, Cambridge.
[3] Permanent address: Department of Physics, Hebrew University.

© American Astronomical Society • Provided by the NASA Astrophysics Data System

1990ApJ...359..164T

quasi-steady situations (Lightman 1974; Pringle 1981). When the disk undergoes rapid expansion or contraction due to the thermal transition, however, this assumption is not always accurate. In this paper, we no longer assume hydrostatic balance, and we explicitly examine how the thermal transition wave propagates in the vertical direction.

In § IV, we study the nonlinear evolution of the thermal instability in irradiated accretion disks. We consider three models: the constant irradiation model, the variable irradiation model, in which irradiation flux varies in proportional to the mass accretion rate onto the compact star, and the abruptly irradiated disk model, in which we abruptly turn on irradiation onto a nonirradiated disk.

In the last section we summarize the numerical results and discuss the observational implications for soft X-ray transients. In particular, we focus on the explanation of the "shoulder" in the light curves of some soft X-ray transients (Priedhorsky and Holt 1987).

II. METHODS OF CALCULATION

a) *Methods of Dynamical Calculation*

In this subsection, we present the methods for the dynamical calculation of an annulus of a given surface density at a fixed radius. The change of the surface density as a consequence of the local evolution will be described in the next subsection.

In analogy with the mass coordinate, $M_r \equiv 4\pi \int_0^r \rho r^2 dr$, which is used in the calculation of stellar models, we introduce the "surface density coordinate," $\Sigma_z \equiv 2 \int_0^z \rho\, dz$, and we use it as the independent Lagrangian variable instead of the vertical coordinate, z. The basic equations are then written as follows: mass conservation is expressed as

$$\frac{dz}{d\Sigma_z} = \frac{1}{2\rho} . \tag{1}$$

The momentum equation in the vertical direction is given by

$$\frac{du}{dt} = -g - 2\frac{dP}{d\Sigma_z} , \tag{2}$$

where u is the vertical component of the velocity and $g \equiv (GM/r^3)z$ is the vertical component of the gravity. The energy equation is written as

$$T\frac{dS}{dt} = \frac{3}{2}\alpha\Omega\frac{P}{\rho} - 2\frac{\partial F_z}{\partial \Sigma_z} \equiv q^+ - q^- , \tag{3}$$

where S denotes the specific entropy, F_z denotes energy transport in the vertical direction, and q^+ and q^- are local heating and cooling rates, respectively. Note that the flux, F_z, includes contributions from both radiative and convective processes (see Paper I).

We integrate the vertical structure of an annulus from the center ($\Sigma_z = 0$) to the surface ($\Sigma_z = \Sigma$ and $z = H_0$). For the central boundary conditions, we have assumed

$$z = u = F_z = 0 . \tag{4}$$

For the surface boundary conditions, we have assumed

$$F_s = \frac{8\sigma T_s^4}{3f_2(\tau_s)} - F_{\rm irr} , \tag{5a}$$

and

$$\delta\tau_s = \delta P_s = 0 . \tag{5b}$$

Here T_s, τ_s, and P_s are the temperature, optical depth, and the local pressure at the surface, $f_2(\tau)$ is a correction factor of order unity (see Appendix A in Paper I), and $F_{\rm irr}$ represents the external irradiation flux. The latter condition of equation (5b) is the planar equivalence to the spherical surface condition: $\delta P/P = -4\delta r/r$ (see Cox and Guili 1968). In the present paper, we take the surface to be at $\tau_s = \frac{2}{3}$ (see $\tau_s = 0.01$ in Paper I). Thus, the external pressure is kept constant during the dynamical evolution. We do not allow mass loss from the disk in this paper.

The methods for solving this system of equations are very similar to those for stellar models (e.g., Kutter and Sparks 1972; Tuchman, Sack, and Barkat 1978), except for the different functional forms for gravity [$g(z) \propto z$ in a disk, while $g(r) \propto r^{-2}$ in a star], and the different kinds of energy sources (viscous heating in a disk, nuclear reactions in a star).

The above differential equations were replaced by difference equations and solved for u, z, P, T, ρ, and F_z as functions of the surface mass (Σ_z) and time, using Henyey's iterative scheme (Henyey, Forbes, and Gould 1964). The time differences were chosen to be a mixture, specified by the parameter θ, between backward ($\theta = 0$; completely explicit) and forward ($\theta = 1$; completely implicit) differences relative to the time at which the mass differences are computed (Richtmyer and Morton 1967). For $0.5 < \theta < 1.0$, high-overtone modes are artificially dampened (Appenzeller 1970), thus permitting relatively large time steps. For $0.0 < \theta < 0.5$, an artificial amplification of these high-overtone modes occurs imposing a small time step. We choose $\theta = 0.55$ to ensure numerical stability together with high accuracy.

b) *One-Zone Torus Evolution*

In this paper, we prescribe the temporal changes in the surface mass density following the one-zone model by MO83. In this model, we approximate a disk as a one-zone isolated annulus (or torus). Although by assumption this model cannot reproduce the global behavior, such as radial propagation of thermal waves, it can follow the basic time-dependent behavior of an annulus (torus) associated with energy imbalance (thermal instability) or mass-flow imbalance (between the mass input rate and the mass output rate).

The basic equation is derived by combining the conservation of mass and angular momentum in the radial direction:

$$\frac{d\Sigma}{dt} = -2\left(\frac{r_R}{\Delta r_R}\right)^2 \frac{W - W_0}{(GMr_R)^{1/2}} . \tag{6}$$

Here r_R and Δr_R represent the radius and the radial width of an annulus, respectively, $W = 2\int_0^{H_0} \alpha P\, dz$ is the integrated viscous stress, W_0 is the integrated stress corresponding to the given mass input rate, $\dot{M}_0$,

$$W_0 = \frac{\dot{M}_0 \Omega_R}{2\pi} , \tag{7}$$

and $\Omega_R = (GM/r_R^3)^{1/2}$.

The change in Σ, $\delta\Sigma$, is then distributed to each calculation grid in proportion to the surface density (mass) at that point.

III. DYNAMICAL EVOLUTION OF A TORUS WITH NO EXTERNAL IRRADIATION

a) *General Behavior*

Results of the dynamical calculations of a one-zone torus with no external irradiation are displayed in Figures 1–3.

© American Astronomical Society • Provided by the NASA Astrophysics Data System

1990ApJ...359..164T

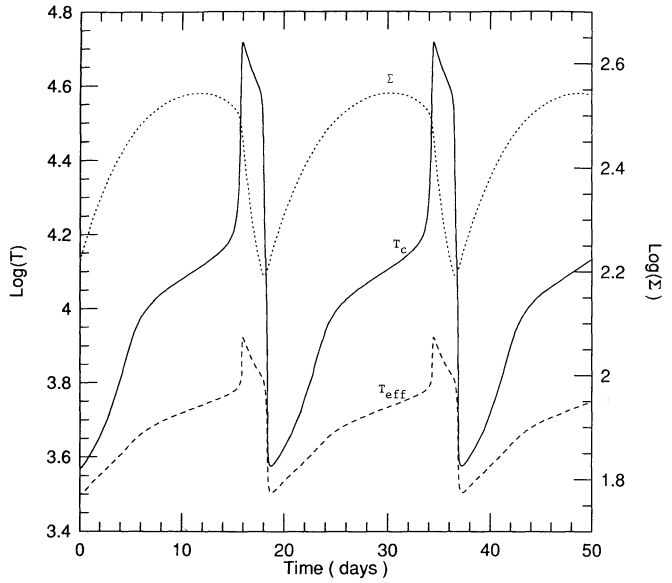

FIG. 1.—Time evolution of an unheated one-zone torus: log T_c (*solid line*), log T_{eff} (*dashed line*), and Σ (*dotted line*). We assume $\alpha = 0.1$.

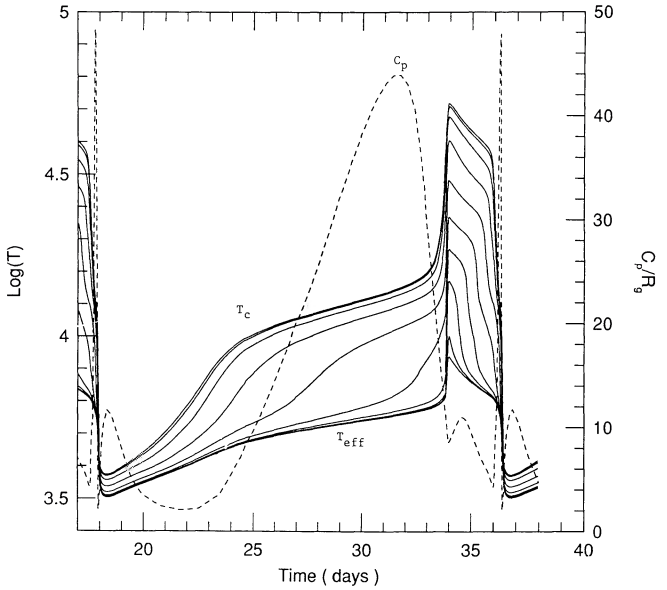

FIG. 3.—Temperature variations at several values of Σ_z (*solid lines*) and C_p as a function of time.

Figure 1 illustrates the time evolution of the effective temperature (*dashed line*), the central temperature (*solid line*), and the surface density (*dotted line*), Figure 2 displays the evolutionary trajectory of the same model together with the thermal equilibrium curves in the (log Σ, log T_c)-plane and the (log Σ, log T_{eff})-plane, respectively, and Figure 3 depicts the time variation of the temperature at different Σ_z (*solid lines*) and of the specific heat, C_p, at $\Sigma_z = z = 0$ (*dashed lines*) on an extended scale.

We assumed $\alpha = 0.1$ and adopted a mass input rate of $\dot{M}_0 = 2.0 \times 10^{17}$ g s^{-1} ($= 10^{-8.5}\ M_\odot$ yr^{-1}), which corresponds to log $T_{eff} \simeq 3.81$ at log r(cm) = 10.5. Since the steady solution resides in the thermally unstable middle branch of the

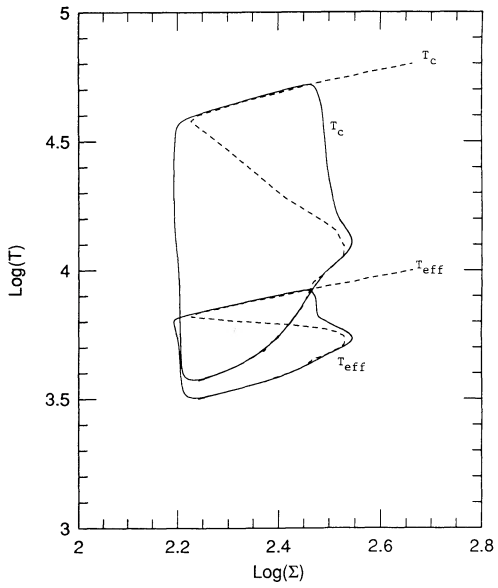

FIG. 2.—Evolutionary trajectory of an unheated one-zone torus in the (log Σ, log T) plane. Thermal equilibrium curves are also indicated by dashed lines.

thermal equilibrium curve (see Fig. 2), the disk should and does exhibit relaxation oscillations between the upper and the lower stable branches. The period of one oscillation is ~ 18 days.

We distinguish five stages as follows (see Figs. 1 and 3):

1. The low state (quiescence): both T_c (also T_{eff}) and Σ increase, while C_p goes through a minimum. The duration is ~ 6 days (day 18 to day 24 in Figs. 1 and 3).

2. The early rise phase (or the stagnation stage): $T_c(T_{eff})$ increases slowly, while Σ is almost constant and C_p goes through a maximum. This stage lasts ~ 9 days (day 24 to day 33 in Figs. 1 and 3).

3. The rapid rise phase: $T_c(T_{eff})$ increases, while Σ and C_p decrease. The time scale is typically a half day.

4. The high state: both $T_c(T_{eff})$ and Σ decreases, while C_p goes through a small maximum. The duration is ~ 2 days.

5. The decay phase: $T_c(T_{eff})$ decreases, while Σ increases and C_p goes through a brief sharp maximum. The time scale is a half-day.

b) *Low State*

In the low state, the evolution of the torus is determined by the viscous process. The duration of the low state is thus approximately given by the viscous time scale in the cool state. From equation (6), we have

$$\tau_{vis,c} \equiv \frac{dt}{d\ln\Sigma} \sim \frac{1}{2}\left(\frac{\Delta r_R}{r_R}\right)^2 \frac{\Sigma}{W_0}\,(GMr_R)^{1/2}\,, \tag{8}$$

where we assumed $W \ll W_0$ in the low state. Since W_0 is a function only of the external parameters ($\dot{M}_0$), the quiescent time scale is independent of T_c; i.e., the evolution is controlled by the external parameter ($\dot{M}_0$). The integrated viscous stress, W_0, is evaluated by

$$W_0 = 2\int_0^{H_0} \alpha P\,dz \sim \alpha\,\frac{R_g}{\mu}\,T_{c,0}\,\Sigma_0\,, \tag{9}$$

where R_g is the gas constant, μ is the mean molecular weight, and $T_{c,0}$ and Σ_0 are values of T_c and Σ corresponding to the steady model determined by $\dot{M}_0$. We thus have the time scale

© American Astronomical Society • Provided by the NASA Astrophysics Data System

1990ApJ...359..164T

in the quiescent phase given by $\tau_Q \sim \tau_{vis,c}(\Delta \log \Sigma/0.4)$, or

$$\tau_Q \sim 8.0(\text{days})\left(\frac{\alpha}{0.1}\right)^{-1}\left(\frac{T_{c,0}}{10^{4.2}}\right)^{-1}\left(\frac{\Delta \log \Sigma}{0.4}\right) \times \left(\frac{r_R}{10^{10.5}}\right)^{1/2}\left(\frac{\Delta r_R/r_R}{0.3}\right)^2, \quad (10)$$

where the factor ($\Delta \log \Sigma/0.4$) comes from the fact that on the viscous time scale Σ increases by a factor e ($\log e \approx 0.4$). For $T_{c,0} \sim 4.2$ and $\Delta \log \Sigma \sim 0.3$, we get $\tau_Q \sim 6$ days, in good agreement with the calculated value.

In the low state, the disk evolves along the lower branch of the equilibrium curves toward the large Σ direction. The low state ends when the disk reaches the lower turning point (lower kink) between the cool branch and the middle branch. One remark concerning the position of the lower kink is in order. In the present calculation, we find the transition temperature to be $\log T_{\rm eff} \sim 3.7$–$3.8$. Some previous calculations found a lower transition temperature; e.g., $\log T_{\rm eff} \sim 3.3$–$3.4$, because of an optically thin branch (Cannizzo, Wheeler, and Ghosh 1982; MO83), or the opacity of the H_2O molecule (Cannizzo and Wheeler 1984; Duschl 1986*a*). Since the shape of the thermal equilibrium curve is rather sensitive to the detailed physics, the methods of calculating convection, the adopted opacity table, and in particular the prescription for the viscosity parameter α, it is difficult to fix the equilibrium curves at this moment.

In full-disk calculations, the duration of the low state will increase, because the one-zone torus model cannot include global effects; that is, the matter added at the outer edge of the disk needs the viscous time scale to reach the inner edge.

c) *Early Rise Phase*

When the evolutionary path in Figure 2 approaches the lower kink, the system enters the stagnation stage. In this stage, the increases of Σ and T_c are suppressed due to the increase in C_p in the partial ionization zone (see Fig. 3). To understand the change from the low state to the stagnation stage, it might be helpful to compare the viscous time scale and the thermal time scale. Usually we have $\tau_{\rm vis} \gg \tau_{\rm th}$ because $\tau_{\rm vis} \sim (r/H_0)^2\tau_{\rm th}$ (Lightman 1974), so the disk tends to approach the thermal equilibrium state on the thermal time scale. When the stagnation begins, however, $\tau_{\rm th}$ grows rapidly owing to the ionization of the hydrogen and helium, and becomes comparable or even longer than $\tau_{\rm vis}$. The thermal time scale is given by (Mineshige 1988)

$$\tau_{\rm th} \sim \frac{\eta}{\alpha\epsilon}\left(\frac{r^3}{GM}\right)^{1/2}, \quad (11)$$

where $\eta \equiv C_p/(R_g/\mu)$, $\epsilon \equiv |(Q^+ - Q^-)/Q^+| (< 1)$, and Q^+ and Q^- are the vertical integrals of the energy gain (q^+) and energy loss (q^-), respectively. Numerically we find

$$\tau_{\rm th} \sim 12.0(\text{days})\left(\frac{\alpha}{0.1}\right)^{-1}\left(\frac{\epsilon}{0.1}\right)^{-1}\left(\frac{\eta}{20}\right)\left(\frac{r_R}{10^{10.5}}\right)^{1.5}. \quad (12)$$

For typical parameters found in the early rise phase, $\eta \geq 20$ and $\epsilon \leq 0.1$, $\tau_{\rm th} > \tau_{\rm vis}$ (see eq. [10]). Hence the duration of the stagnation stage, $\tau_{\rm stag}$, is determined by the thermal time scale, not by the viscous time scale;

$$\tau_{\rm stag} \approx \tau_{\rm th}\left(\frac{\Delta \log T_c}{0.4}\right) \sim 12 \text{ (days)}, \quad (13)$$

for $\eta \sim 40$, $\epsilon \leq 0.05$ (Fig. 2), and $\Delta \log T_c \sim 0.1$ (Fig. 1), in reasonable agreement with the calculated value.

Note that the increase of temperatures at different Σ_z is not homologous (Fig. 3). As time goes on, the partial ionization zone extends from the central plane toward the surface, suppressing the rapid change in the temperature. When the hydrogen and helium are entirely ionized, the stagnation stage is terminated, and the system enters the rapid rise phase. Then we have again $\tau_{\rm th} \ll \tau_{\rm vis}$. In full-disk calculations $\tau_{\rm stag}$ will be much reduced, because $\tau_{\rm stag}$ is shorter at inner radii and thus the rapid rise phase is initiated at relatively inner portions of the disk.

From the observational point of view, this stagnation stage is responsible for the UV delay in the early rise of some dwarf novae (Mineshige 1988, and references therein). In § V we will discuss the observational consequences in detail.

d) *Rapid Rise Phase*

The rise time scale is the time in which T_c increases from $\log T_c = 4.1$ to 4.7 ($\Delta \log T_c \simeq 0.6$) on the thermal time scale (eq. [11]);

$$\tau_{\rm rise} \approx \tau_{\rm th}\left(\frac{\Delta \log T_c}{0.4}\right) \sim 0.3(\text{days}), \quad (14)$$

for $\eta = 5$ and $\epsilon = 1$, consistent with the calculated value. It should be noted that the increase in $\log T_c$ ($\Delta \log T_c \sim 0.6$) is much bigger than that in $\log T_{\rm eff}$ ($\Delta \log T_{\rm eff} \sim 0.1$), because the ratio of T_c to $T_{\rm eff}$ is a function of the optical thickness ($T_{\rm eff} \sim T_c/\tau^{1/4}$), and τ increases with increase of T_c. The emission lines are observed to suddenly disappear in the course of this rapid transition.

In Figure 4 we display the time evolution of the flux (F_z) at different Σ_z. We can see that the rate of change in the logarithm of F_z, $\delta \log F_z$, is approximately the same for each trajectory, i.e., $\delta F_z/F_z \sim$ constant, regardless of Σ_z. In contrast, Figure 3 shows that $\delta \log T (\propto \delta T/T)$ is not constant for different curves. This feature was already pointed out by the linear analysis of Saio, Cannizzo, and Wheeler (1987). Now we

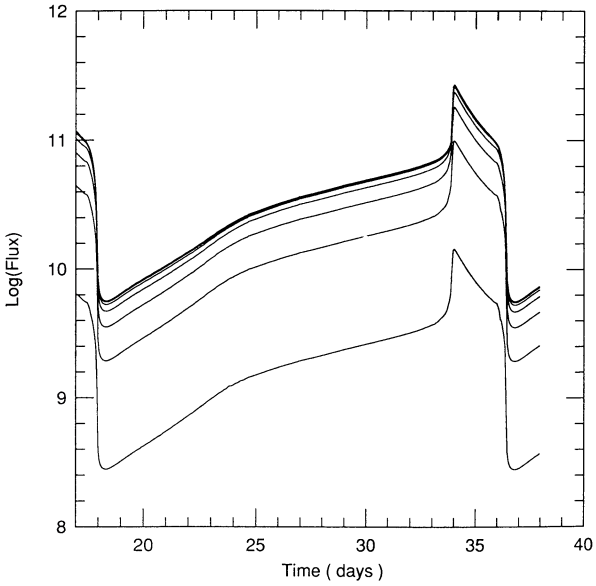

FIG. 4.—Same as Fig. 3, but time changes in $\log F_z$ at several points of Σ_z.

© American Astronomical Society • Provided by the NASA Astrophysics Data System

1990ApJ...359..164T

confirm this feature also in the nonlinear regimes. The approximation of constant $\delta F_z/F_z$ adopted by Mineshige and Osaki (1983, 1985) is justified.

e) High State

In the high state, $W \gg W_0$, and hence the effect of the mass input is almost negligible in the outburst phase. The evolution of the torus is then determined by the disk structure itself and not by the external effect, as is the case in the low state (see § III*b*). The duration of the high state is of order the viscous time scale in the hot state, which is

$$\tau_{\mathrm{vis},h} \sim 3.1(\mathrm{days})\left(\frac{\alpha}{0.1}\right)^{-1}\left(\frac{T_c}{10^{4.6}}\right)^{-1}\left(\frac{r_R}{10^{10.5}}\right)^{1/2}\left(\frac{\Delta r_R/r_R}{0.3}\right)^{2}. \tag{15}$$

Since the surface density decreases as $\Delta \log \Sigma \approx 0.3$,

$$\tau_{\mathrm{burst}} \simeq \tau_{\mathrm{vis},h}\left(\frac{\Delta \log \Sigma}{0.4}\right) \approx 2.4(\mathrm{days}), \tag{16}$$

in agreement with the calculations.

f) Decay Phase

The downward transition is triggered when the disk reaches the upper turning point in the thermal equilibrium curve. The time scale for the decay is estimated using equation (12) to be $\tau_{\mathrm{decay}} \sim 1$ day for $\eta = 20$. We should note that stagnation is not seen in the decay phase, because the peak of η (or C_p) occurs when the disk is far from the thermal equilibrium state (see Figs. 2 and 3) so that the parameter ϵ in equation (11) is large. In contrast, in the early rise phase η reaches its peak when the disk is in the quasi-thermal equilibrium state; i.e., $\epsilon \ll 1$.

g) Scaling Law

The radial dependence of the thermal equilibrium curves have been calculated by many groups. It is shown that the basic shape of the curves and the temperature of the turning points are rather insensitive to the radius and the value of α, while the surface density of the turning points is dependent on r as $\Sigma_{\mathrm{crit}} \propto r$, and also on α approximately as; $\Sigma_{\mathrm{crit}} \propto \alpha^{-0.8}$ (see, e.g., MO83). Using these facts, we can rescale the results obtained in previous subsections to different radii.

From the steady state relation, we have

$$T_{\mathrm{eff}}^0 \simeq 10^{3.81}\left(\frac{\dot{M}_0}{10^{17.3}}\right)^{1/4}\left(\frac{r}{10^{10.5}}\right)^{-3/4}. \tag{17}$$

Here T_{eff}^0 represents the effective temperature of the steady disk model for a given $\dot{M}_0$. The mass-transfer rate which gives the same T_{eff}^0 at the radius, $r = 10^{1.0} r_{10}$ cm, is then derived as

$$\dot{M}_0 = 10^{15.8} {r_{10}}^3. \tag{18}$$

Similarly, the value of α which gives the same Σ_{crit} as in the previous subsections is

$$\alpha = 10^{-1.625} {r_{10}}^{1.25}. \tag{19}$$

The viscous time scale is thus altered as (see eqs. [10] and [15])

$$\tau_{\mathrm{vis}} \propto \alpha^{-1} r^{1/2} \propto {r_{10}}^{-0.75}, \tag{20}$$

and the thermal time scale is (see eq. [12])

$$\tau_{\mathrm{th}} \propto \alpha^{-1} r^{3/2} \propto {r_{10}}^{0.25}. \tag{21}$$

For instance, the model in Figures 1 and 2 ($\log r = 10.5$, $\log \dot{M}_0 = 17.3$, and $\alpha = 0.1$) is rescaled to a model with $\log r = 10.0$, $\log \dot{M}_0 = 15.8$ and $\alpha = 10^{-1.625}$ (≈ 0.025). The quiescent and outburst durations are increased by a factor $\sim 10^{0.375} \approx 2.3$, and the rise and decay time scales are decreased by a factor $\sim 10^{0.125} \approx 1.3$.

h) Summary of Nonirradiated Models

1. The dynamical evolution of the nonirradiated one-zone torus is consistent with the vertically averaged models. The approximation of $\delta F_z/F_z \sim$ constant is justified.

2. The stagnation stage is also clear in the dynamical calculations. The vertical location of high C_p travels from the center to the surface with time and so strengthens the effect of stagnation even more.

IV. DYNAMICAL EVOLUTION OF AN IRRADIATED TORUS

a) Model Descriptions

We assume that the irradiation flux is proportional to the X-ray luminosity, L_X,

$$F_{\mathrm{irr}}(t) \equiv \sigma[T_{\mathrm{irr}}(t)]^4 = C\frac{L_X(t)}{2\pi r_R^2}, \tag{22}$$

where C is a constant representing the fraction of the X-ray energy which is caught by the outer disk. In Paper I, we have estimated that $C \sim 10^{-2}$ if the disk is exposed to direct irradiation, and $C \leq 10^{-4}$ if the outer portions of the disk are shaded by the inner portions of the disk and so indirect heating, such as scattering of the direct irradiation by an accretion disk corona, is dominant (Meyer and Meyer-Hofmeister 1984). Physical parameters adopted in this section are the same as those in § III: $\dot{M}_0 = 2.0 \times 10^{17}$ g s^{-1}, $\alpha = 0.1$, and $\log r_R$ (cm) = 10.5.

In this paper, we consider the following three cases for irradiation.

1. Constant T_{irr} model: $L_X = \mathrm{const.}$, thus T_{irr} is also constant.

2. Variable T_{irr} model: the X-ray luminosity varies in proportion to the mass accretion rate, $\dot{M}_a$,

$$L_X(t) = \frac{GM\dot{M}_a(t)}{R_{\mathrm{in}}}, \tag{23}$$

and

$$\dot{M}_a(t) = \frac{2\pi W(t-\Delta t)}{\Omega_R}, \tag{24}$$

where R_{in} is the inner radius of the disk, and we introduced a time delay, Δt, representing the time for matter at $r = r_R$ to reach $r = R_{\mathrm{in}}$. Using equations (22)–(24), we get

$$T_{\mathrm{irr}}(t) = 10^{3.9}(\mathrm{K})\left(\frac{C}{10^{-4}}\right)^{1/4}\left(\frac{M}{M_\odot}\right)^{-1/4} \times\left[\frac{\dot{M}_a(t-\Delta t)}{10^{17}}\right]^{1/4}\left(\frac{r_R}{10^{10.5}}\right)^{-1/2}\left(\frac{R_{\mathrm{in}}}{10^6}\right)^{-1/4}. \tag{25}$$

3. Abruptly irradiated disk model: the irradiation is abruptly turned on,

$$T_{\mathrm{irr}}(t) = \begin{cases} 0 & \text{for } t < 0\ ; \\ T_{\mathrm{irr},0} & \text{for } t \geq 0\ . \end{cases} \tag{26}$$

Here $T_{\mathrm{irr},0}$ is an input parameter.

© American Astronomical Society • Provided by the NASA Astrophysics Data System

1990ApJ...359..164T

b) Constant T_{irr} Model

First we examine the case for which T_{irr} is constant in time. Results of this model are consistent with our expectation derived from the thermal equilibrium curves (Paper I); that is, when the irradiation temperature exceeds the critical value of $T_{irr}^{crit} \sim 10{,}000$ K, the disk is stationary, because the thermally unstable branch disappears. When the irradiation is moderately strong, say $T_{irr} = 4500$ K, the thermal limit cycle is expected but with smaller amplitude and shorter periods than the nonirradiated model.

In Figure 5 we illustrate the time evolution of a model with $T_{irr} = 6000$ K; the dashed line represents T_{eff}, the solid line T_c, and the dotted line Σ, respectively. The corresponding value of C is from equation (25),

$$C = 10^{-4.4}\left[\frac{M_a(t-\Delta t)}{10^{17}}\right]^{-1}\left(\frac{r_R}{10^{10.5}}\right)^2 . \quad (27)$$

Note C is no longer constant in this model, because $\dot{M}_a$ is time dependent. We thus use T_{irr} as a parameter to describe the model instead of C.

We can summarize several noteworthy features in Figure 5. First of all, the low state merges with the stagnation stage: the temperature is always kept around log $T_{eff} \sim 3.8$, and so the partial ionization zone is always present in the disk. This is a result of the continuous heating by the external irradiation. The time variation in log T_{eff}, Δ log T_{eff}, and so the amplitude of the light variation are thus much smaller than in Figure 1; Δ log $T_{eff} \sim 0.1$ (vs. $\simeq 0.4$ in Fig. 1). The time variation in log T_c is also reduced, but there is still a factor ~ 4 difference; Δ log $T_c = 0.6$ (vs. $\simeq 1.2$ in Fig. 5). These two points are expected from the shape of the thermal equilibrium curves (Fig. 1 in Paper I).

Second, there is one interesting feature concerning the maximum temperature: even though we include an additional heating source in this model, the maximum value of T_c is smaller in Figure 5 than that in Figure 1. This is because the critical value of Σ, where the upward transition is initiated, decreases with the increase of T_{irr} so that the corresponding value of T_c also decreases on the upper branch. This feature is, however, not observable, because the maximum values of T_{eff} are almost identical in Figures 1 and 5. The effective temperature for a given value of Σ increases in the irradiated disk, and this increase cancels the decrease of Σ at the transition point.

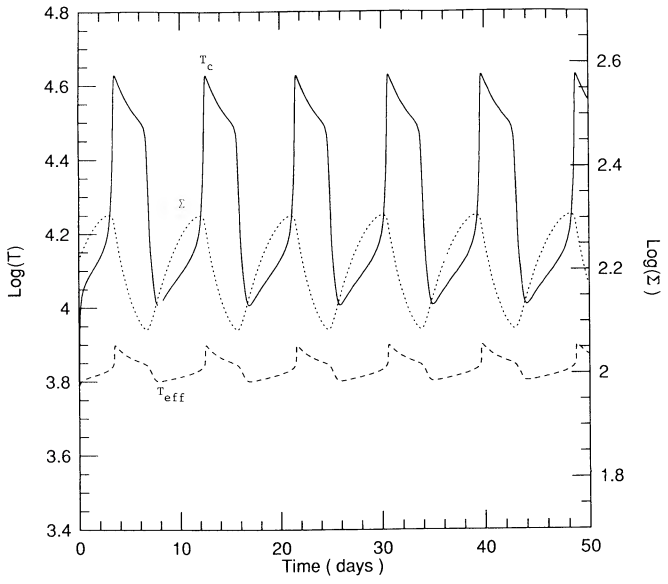

FIG. 5.—Time evolution of a heated one-zone torus. The irradiation temperature is assumed to be constant and $T_{irr} = 6000$ K.

Third, the quiescent time scale decreases to ~ 4 days. To understand this, we define the effective α by rewriting the equation of energy conservation (integral of eq. [3]),

$$F_s = \tfrac{3}{4}W\Omega + F_{irr} \equiv Q_{vis}^{+} + Q_{irr}^{+} , \quad (28)$$

as

$$F_s = \left(\frac{\alpha_{eff}}{\alpha}\right)Q_{vis}^{+} . \quad (29)$$

Since $F_{irr} > 0$, we find $\alpha_{eff} > \alpha$. From equation (10), the increase of the effective value of α results in the decrease of the quiescent duration. On the other hand, the outburst duration increases to ~ 4 days owing to the *decrease* of T_c in the high state (eq. [15]). As a result, the duty cycle, $\beta \equiv \tau_{burst}/(\tau_Q + \tau_{burst})$, increases when moderately strong external irradiation is present. In the limit of strong irradiation, $F_{irr} \to \infty$, $\beta \to 1$.

To sum up, the light curves of moderately irradiated disks in the thermally unstable condition are more sawtooth-shaped than nonirradiated cases due to the truncation of the stagnation phase and the increase in the duty cycle. The bursts are characterized by small-amplitude (~ 1 mag) light fluctuations with quasi-periodic upward and downward motion. These general trends are very reminiscent of the typical light curves of soft X-ray transients (discussed in detail later).

c) Variable T_{irr} Model

In this model, we allow F_{irr} to change in proportion to $\dot{M}_a$. We fix the value of C in equation (25) to be $C = 10^{-5}$; thus the irradiation temperature is T_{irr} (K) $\approx 6500\,(\dot{M}_a/\dot{M}_0)^{1/4}$. In actual calculations, we first run the program without taking account of irradiation for a period of one limit cycle, and then we turn on the irradiation.

First we take the time delay to be 2 days in equation (24), which is much shorter than a period of one (nonirradiated) limit cycle ~ 18 days. In Figure 6 we display the temporal evolution of such a model after the limit-cycle behavior is established; the solid line represents the time evolution of T_c, the dotted line represents Σ, the dashed line represents T_{eff}, and the dash-dot line T_{irr}, respectively. We see that the effect of the irradiation is only appreciable at maximum light. In fact, the temperature, T_c or T_{eff}, roughly decreases to the same minimum values obtained in the nonirradiated model (Fig. 1). The period of one cycle is slightly reduced; $P \simeq 15$ days. The outburst duration is increased, similarly to the constant T_{irr} model. This increase is, however, due not only to the decrease of T_c but also due to the delay heating by the irradiation. The time variation of T_{eff} therefore has two peaks per one period: the former is caused by the thermal instability and the latter is caused by the external irradiation. The curve of T_c, on the other hand, has only one peak per one period, because the external irradiation can heat up only the surface layer (T_{eff}) and scarcely affects the interior structure (T_c).

In Figures 7 and 8, we present the results of models with longer time delays; $\Delta t = 4.0$ days in Figure 7 and 8.0 days in

© American Astronomical Society • Provided by the NASA Astrophysics Data System

1990ApJ...359..164T

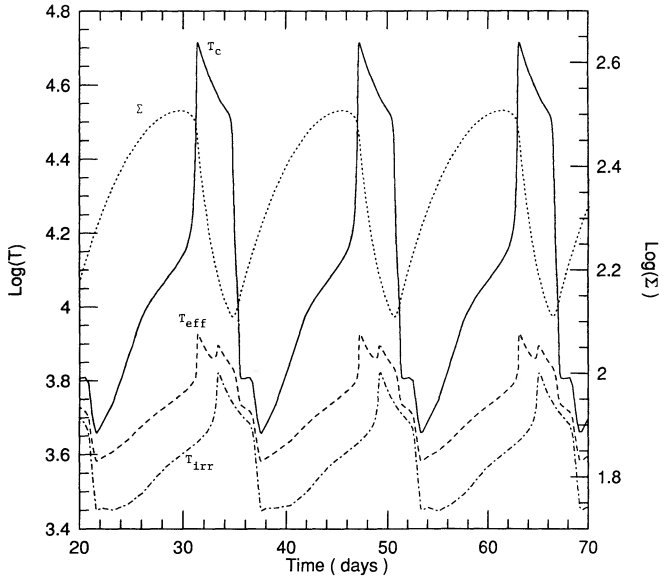

FIG. 6.—Time evolution of a heated torus. The irradiation is a function of the mass accretion rate, $\dot{M}_a$, with the proportionality constant $C = 10^{-5}$. We introduced a time delay of $\Delta t = 2.0$ days.

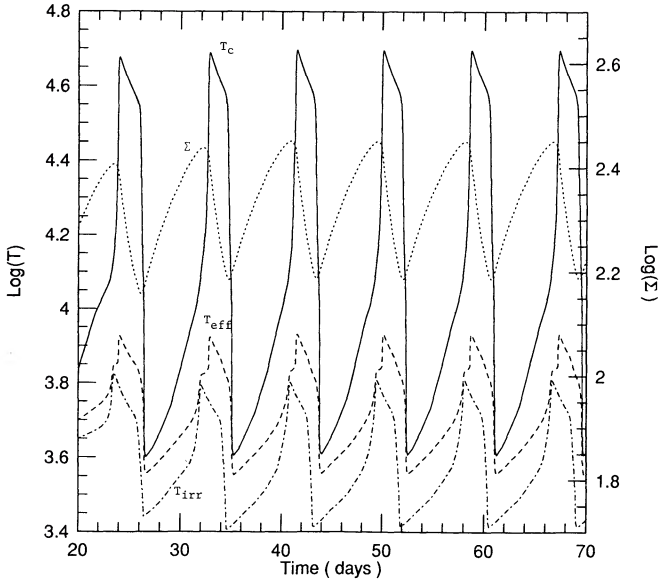

FIG. 8.—Same as Fig. 6, but for $\Delta t = 8.0$ days

Figure 8. Note that 8 days was the period for the fixed T_{irr} model. Figure 7 looks similar to Figure 6, except that not only T_{eff} but also T_c has two peaks during one period in this model. Here we thus distinguish two distinct mechanisms for the thermal transition of the disks. One is the ordinary "intrinsic thermal instability," invoked by the change of the surface density, and the other is the "forced thermal instability," which is induced by the turn-on or turn-off of the external heating. It might be kept in mind that in the low state (and only in the low state), the central temperature is sensitive to the irradiation (Paper I).

When we increase Δt even more, then the period of the limit cycle is completely synchronized with Δt (Fig. 8). In other words, the thermal limit cycle is controlled by the "forced thermal instability." We also calculated models with $\Delta t = 10$, 12, and 14 days, and we found that one period of the limit cycle is exactly the same as Δ_t.

When we increase the parameter C, the effects of irradiation becomes much more evident. Figure 9 depicts the time evolution of the heated disk with $C = 5 \times 10^{-5}$, corresponding to $T_{irr} \approx 7000$ (K) $(\dot{M}_a/\dot{M}_0)^{1/4}$. The other parameters are the same as the model in Figure 7 ($\Delta t = 4$ days). The period is ~ 20 days. The standstill (plateau seen in the decay phase) is clear in this model because of the larger C. We also find that $T_{eff} \approx T_{irr}$ throughout outburst cycles in this model (dashed and dot-dash lines in Fig. 9). The duty cycle is $\beta = 0.86$, and $\Delta \log T_{eff} \sim 0.1$.

d) Abruptly Irradiated Disk Model

In previous models we have assumed that the irradiation changes more or less smoothly in accordance with the modula-

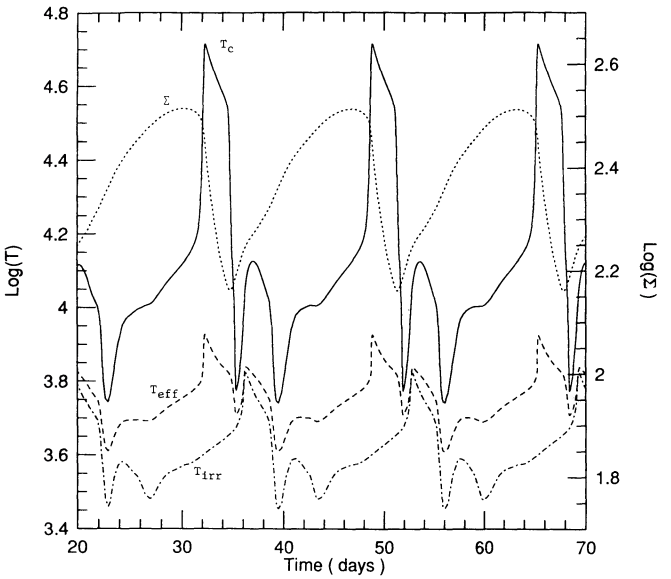

FIG. 7.—Same as Fig. 6, but for $\Delta t = 4.0$ days

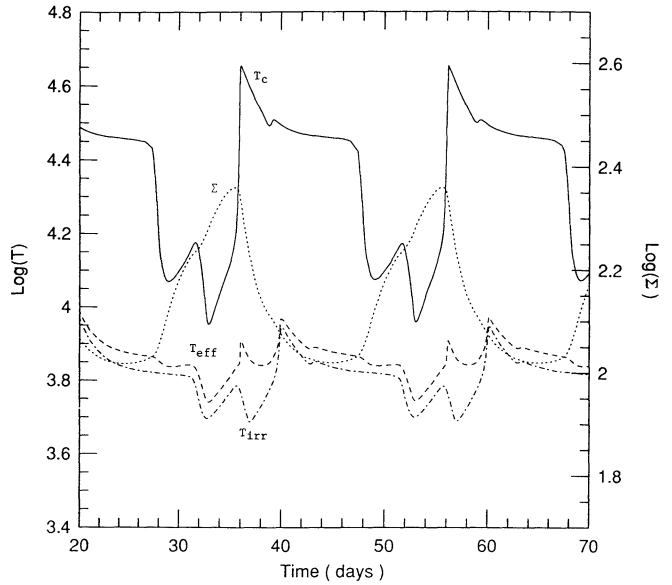

FIG. 9.—Same as Fig. 7 ($\Delta t = 4.0$ days), but for $C = 5 \times 10^{-5}$

© American Astronomical Society • Provided by the NASA Astrophysics Data System

1990ApJ...359..164T

tion in $\dot{M}_a$. In an actual system, however, the disk might be suddenly exposed to a strong irradiation. Suppose in the decay phase of the soft X-ray transients, the cooling front moves inward leaving behind a cool region. Since H_0/r decreases with the radius as $H_0/r \propto r^{1/2}$ in the cool state, when the cooling wave reaches and thins the inner regions of the disk, the outer portions of the disk can be suddenly exposed to the irradiation from the inner part of the disk or from the neutron star.

The results of the simulation of such a time dependence are shown in Figure 10. We take $T_{\rm irr,0} = 6000$ K and assume that Σ is kept constant, because the time scale of the expansion of the disk is of order the sound crossing time scale (or dynamical time scale),

$$\tau_{\rm cs} \sim \frac{H_0}{C_s} \sim 5.0 \times 10^2 ({\rm s}) \left(\frac{M}{1\ M_\odot}\right)^{1/2} \left(\frac{r_R}{10^{10.5}}\right)^{3/2} , \quad (30)$$

which is much shorter than the viscous time scale, on which Σ varies.

The effective temperature suddenly rises in response to the abrupt heating even faster than does the central temperature. Figure 10 shows that the rise time scale of $T_{\rm eff}$ is ~ 0.03 days, much shorter than the thermal time scale of the bulk of the disk, $\tau_{\rm th} \sim 0.3$ day for $\epsilon = 1$ and $\eta = 5$ (eq. [12]), while T_c requires $\tau_{\rm th}$ to increase. Obviously the hydrostatic balance is no longer achieved during the transition because of the temperature inversion; $T_c < T_{\rm eff}$ (see eq. [2]). In this calculation, we fix the surface density; however, if we had not, we naively expect a mass loss from the surface of the disk, causing the formation of an accretion disk corona. The time-dependent behavior of the Compton wind–heated accretion disk was investigated by Shields *et al.* (1986) (see also Schwarzenberg-Czerny 1989). They demonstrated that if the wind mass-loss rate changes sensitively to the mass accretion rate through the inner edge of the disk, the disk exhibits nonlinear oscillation.

e) Scaling Law

For the irradiated model, a scaling law can be obtained similar to that for the nonirradiated model (see § III*g*). The results obtained in this section ($\log r_R = 10.5$ and $\alpha = 0.1$) can be rescaled to different radii. In addition to the scaling laws found in § III*g*, we get the following relations for the case with irradiation. For the constant $T_{\rm irr}$ model in § III*c*, the irradiation temperature is invariant to have a functional dependence of

$$C \propto \dot{M}_a^{-1} r_R^{\ 2} , \quad (31)$$

the scaled model at $r_R = r_{10} 10^{10.0}$ cm, which has the same value of $T_{\rm irr}$ (see eq. [25]), has the value of

$$C = 10^{0.5} C_0 r_{10}^{\ -1} , \quad (32)$$

where C_0 is either 10^{-5} (Figs. 6–8) or 5×10^{-5} (Fig. 9). For the abruptly irradiated disk model, the irradiation temperature is the same as the original value, as it is in the constant $T_{\rm irr}$ model.

For instance, the models in Figures 6–9 ($\log r = 10.5$, $\log \dot{M}_0 = 17.3$, $\alpha = 0.1$, and $C = 10^{-5}$ in Figs. 6–8, and 5×10^{-5} in Fig. 9) can be rescaled to models with $\log r = 10.0$, $\log \dot{M}_0 = 15.8$, $\alpha \approx 0.06$, and $C \simeq 3.2 \times 10^{-5}$ for the models in Figures 6–8, and $C \simeq 1.5 \times 10^{-4}$ for the model in Figure 9.

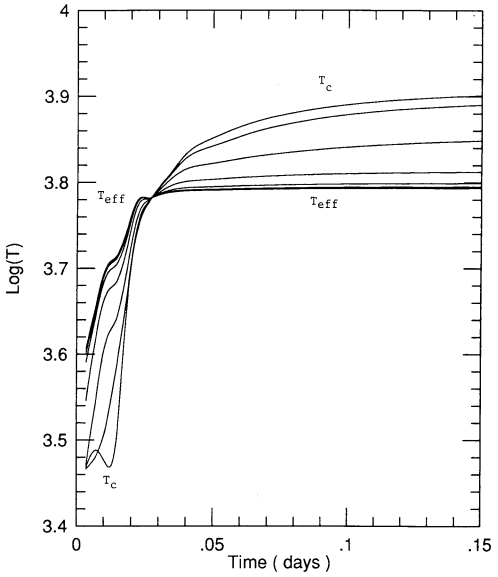

FIG. 10.—Time evolution of an abruptly irradiated one-zone torus

f) Summary of Irradiated Models

In the following, we summarize the results of the irradiated models.

1. We distinguish two distinct causes of the thermal instability: one is the ordinary "intrinsic thermal instability" which is valid also in the nonirradiated models, and the other is "forced thermal instability," which is induced by the switch-on or switch-off of external irradiation.

2. For moderately strong irradiation ($T_{\rm irr} \leq 10{,}000$ K), the limit cycle is triggered by the "intrinsic thermal instability." Because of the presence of the irradiation, the quiescent period is in general reduced due to the increase of $\alpha_{\rm eff}$ (eq. [29]), while the outburst duration is increased.

3. When the disk is exposed to strong irradiation on a short time scale, then the disk suffers a "forced thermal instability." The period of the limit cycle is determined by the time delay in response of the irradiation flux to the structural change of a torus, not by the intrinsic period of the instability of the torus.

4. The time variation in $T_{\rm eff}$ in the variable $T_{\rm irr}$ models have shoulders in the decay phase (evident in Fig. 9) induced by the delayed heating of the irradiation.

5. If the disk is abruptly exposed to external irradiation, the surface temperature goes up on a time scale much shorter than the thermal time scale (of the center), while the central temperature increases on the thermal time scale. During the transition, the disk is not in the hydrostatic balance.

V. DISCUSSION AND CONCLUSIONS

a) UV Delay and the Stagnation Stage

In the early rise phase of outbursts in some dwarf novae, the UV rise is delayed behind the optical rise, a phenomenon explained by the stagnation in the evolution (§ III*c*). In full-disk calculations, the propagation of the thermal transition wave shortens the duration of the stagnation stage to the order of 1 day (Mineshige 1988).

Two distinct types of outbursts are obtained in the full-disk calculations (see, e.g., Smak 1984; Mineshige and Osaki 1985; Cannizzo, Wheeler, and Polidan 1986). In the outside-in outbursts, the brightening of the disk is initiated at the outer portions of the disk, and then the heating wave propagates inward, transforming the inner cool regions successively into

© American Astronomical Society • Provided by the NASA Astrophysics Data System

1990ApJ...359..164T

the hot state. In the inside-out outbursts, the thermal instability is triggered in the inner portions of the disk, and the heating wave propagates outward from the ignition radius. The stagnation appears only in the outside-in burst. This explains the different photometric and spectroscopic behavior between the two different groups of outbursts (Smak 1987; Verbunt 1987).

Recently la Dous (1989) investigated the published observations of the size of the Balmer jump in dwarf novae and found that in one type of outbursts (which seem to be inside-out outbursts), the Balmer jump is zero throughout the outburst, while in the other (perhaps outside-in outbursts), it is strong in absorption during the rise and gradually declines in the late rise phase. Whether or not a Balmer jump appears depends on the temperature gradient at the surface of the disk; the presence of a Balmer jump indicates the existence of a relatively large temperature gradient. In Figure 3, we see that the temperature gradient in the surface zone (indicated by the distance between the line for $T_{\rm eff}$ and the adjacent line) increases in the rise phase and reaches its maximum when the upward transition is completed, because the opacity, κ, has a peak at $\log T \sim 4.1$. This feature may be responsible for presence of a Balmer jump in the early rise phase of some outbursts (i.e., outside-in outbursts).

b) *Duty Cycle and Amplitude*

The values obtained for the duty cycle and amplitude are different between the fixed irradiation model and the variable irradiation model. In the former model, as $T_{\rm irr}$ increases, the amplitude is drastically decreased and the duty cycle, β, increases, $\tau_{\rm burst} \sim \tau_Q$, whereas in the latter model, the amplitude and duty cycle are almost identical to those in the nonirradiated model, because irradiation is absent in quiescence.

If the surface temperature of a neutron star is almost independent of the mass accretion rate, then the associated $T_{\rm irr}$ is nearly constant in time (unless disk self-shielding occurs), and so the amplitude of the light variations would be much decreased ($\Delta m_V \sim 1$ mag) and β would be close to unity. Similar results are obtained for the variable irradiation model with a higher C ($\sim 5 \times 10^{-4}$), or the model with higher $\dot{M}_0$, because the change in the mass accretion rate turns out to be small in this model. Such features are observed in some low-mass X-ray binaries e.g., 4U1820−30 and 4U1915−05 (Priedhorsky and Holt 1987). We further suggest that our model might explain the 300 day periodicity of the optical and the X-ray variation in Cyg X-1 (Kemp *et al.* 1983; Priedhorsky, Terrell, and Holt 1983).

On the other hand, if the irradiation is a function of the mass accretion rate and is not so strong ($C \sim 10^{-4}$ and $T_{\rm irr} \leq 5000$ K at maximum), then amplitudes are around 4–5 mag and $\beta \ll 1$. Note that the global effect tends to increase amplitudes by 1–2 mag and decrease β significantly. Moreover, if we assign larger α in the high state and lower α in the low state, which is required to reproduce the observed light variations of dwarf novae (Smak 1984; Mineshige and Osaki 1983, 1985), then β is further decreased (eqs. [10] and [15]). The variable $T_{\rm irr}$ model is thus relevant to soft X-ray transients with larger amplitudes (≥ 6 mag) and smaller duty cycles ($\leq 1/10$); such as A0620−00. Aql X-1, and Cen X-4. In these systems, the observed X-ray luminosity varies by several orders of magnitude in the course of outburst-quiescence cycles.

The decay time scales are usually increased by the irradiation heating. This feature is consistent with the suggestion of van Paradijs and Verbunt (1984), who compared the outburst properties of dwarf novae and soft X-ray transients and found that decay time scales are longer in soft X-ray transients.

c) *Standstill in the Light Curves of X-Ray Transients*

The plateau in the light curves of an irradiated torus (Figs. 7 and 9) is reminiscent of the standstill (or the "shoulder") in the observed light curves of neutron star binaries such as 4U1705−44 and 4U1630−47 (Priedhorsky and Holt 1987), and the black hole candidate A0620−00 (Whelan *et al.* 1977); however, several things should be kept in mind. First of all, the irradiation flux should be moderately strong to cause a plateau, but should not be so strong as to suppress the thermal instability. In Paper I, we estimated the required value of C to be $C \leq 10^{-4}$. This value is easily achieved in quiescence and in the decay phase, because the outer cool portions of the disk are shaded by the inner hot regions. At maximum light, in contrast, the outer parts of the disk are not shaded, so a mechanism to trigger the cooling wave is still in question. Wind mass loss from the disk due to the Compton heating (Begelman, McKee, and Shields 1983) or an irradiation instability of the sort discussed in Paper I might provide such a mechanism. Second, we neglect global effects in this paper. In order to accurately evaluate the time delay, which is given *a priori* in our model, the global calculations are indispensable.

d) *Chaos*

Finally, we comment on the requirement for getting chaos in the light curves. We note from Figures 5–9 that for increased time delay Δt the repetition time of the outbursts become identical to the delay time. This is because the increased irradiation triggers a forced thermal instability, amplifying the mass accretion rate. The physical system as we have defined it thus undergoes positive feedback and is stable. It does not undergo a period doubling leading to the onset of deterministic chaos. The latter behavior was found in the models of Livio and Regev (1985), who imposed a negative feedback in a parameterized way in the context of type I X-ray bursts. It remains to be seen whether such negative feedback occurs in realistic systems in a sufficiently strong way to overcome the positive feedback intrinsic to the irradiation process as computed here. Wind mass loss (Begelman McKee, and Shields 1983; Shields *et al.* 1986) is one possibility to induce negative feedback.

e) *Conclusions*

1. We have calculated the nonlinear evolution of the thermal instability in accretion disks. It is concluded that the UV delay and the presence of a Balmer jump detected in some dwarf-nova outbursts (interpreted as outside-in outbursts) may be well accounted for by the disk-instability model.

2. In the constant $T_{\rm irr}$ model with moderate irradiation temperature ($T_{\rm irr} < 10{,}000$ K), the amplitudes of the thermal limit cycles of dwarf-nova type eruptions are reduced to ~ 1 mag, and the duty cycle becomes ~ 1. Similar results are expected in the variable irradiation model with higher $\dot{M}_0$. Both features are actually observed in some X-ray transients. Moreover, the 300 day variation of Cyg X-1 may be explained by our model.

3. In the variable $T_{\rm irr}$ model with smaller $\dot{M}_0$ ($\sim 10^{15}$ g s^{-1}) or smaller C ($\sim 10^{-5}$), the amplitude and the duty cycle are similar to those of nonirradiated models, but the decay time is increased by the heating from the delayed irradiation. The light curves have a plateau in the decline phase from outburst. This might be responsible for the shoulder observed in the light

© American Astronomical Society • Provided by the NASA Astrophysics Data System

1990ApJ...359..164T

curve of A0620−00, and also for similar effects in some X-ray transients containing neutron stars.

4. In the abruptly heated disk, the effective temperature goes up faster than the central temperature, creating a temperature inversion for a time scale much shorter than the thermal time scale. The wind mass loss arising from the rapid heating of the surface might lead to the formation of an accretion corona.

We wish to thank G. A. Shields, E. Vishniac, and M. Huang for their fruitful discussion and critical comments. S. M. is also grateful to D. E. Baldwin, H. Berk, T. Tajima, and other personnel at the Institute for Fusion Studies for their hospitality. Numerical calculations were performed on the Cray X-MP at the University of Texas System Center for High Performance Computing. This research was supported in part by NSF grant 8717166, NASA grant NSG 7232, and US Department of Energy DE-FG05-80 ET53088.

REFERENCES

Appenzeller, I. 1970, *Astr. Ap.*, **5**, 355.
Begelman, M. C., McKee, C. F., and Shields, G. A. 1983, *Ap. J.*, **271**, 70.
Cannizzo, J. K., and Wheeler, J. C. 1984, *Ap. J. Suppl.*, **55**, 367.
Cannizzo, J. K., Wheeler, J. C., and Ghosh, P. 1982, in *Pulsations in Classical and Cataclysmic Variable Stars*, ed. J. P. Cox and C. J. Hansen (Boulder: University of Colorado Press), p. 13.
———. 1985, in *Proc. Cambridge Workshop on Cataclysmic Variables and Low-Mass X-Ray Binaries*, ed. D. Q. Lamb and J. Patterson (Dordrecht: Reidel), p. 307.
Cannizzo, J. K., Wheeler, J. C., and Polidan, R. S. 1986, *Ap. J.*, **301**, 634.
Clarke, C. J. 1987, Ph.D. thesis, Oxford University.
Cox, J. P., and Guili, R. T. 1968, *Principles of Stellar Structure* (New York: Gordon & Breach), § 27.
Duschl, W. J. 1986*a*, *Astr. Ap.*, **163**, 56.
———. 1986*b*, *Astr. Ap.*, **163**, 61.
Henyey, L. G., Forbes, J. E., and Gould, N. C. 1964, *Ap. J.*, **139**, 306.
Hōshi, R. 1979, *Prog. Theor. Phys.*, **61**, 1307.
Huang, M., and Wheeler, J. C. 1989, *Ap. J.*, **343**, 229.
Kemp, J. C., *et al.* 1983, *Ap. J.* (*Letters*), **271**, L65.
Kutter, G. S., and Sparks, W. M. 1972, *Ap. J.*, **175**, 407.
la Dous, C. 1989, *M.N.R.A.S.*, **238**, 935.
Lightman, A. P. 1974, *Ap. J.*, **194**, 419.
Lin, D. N. C., and Shields, G. A. 1986, *Ap. J.*, **305**, 28.
Livio, M., and Regev, O. 1985, *Astr. Ap.*, **148**, 133.
Lyutyi, V. M., and Syunyaev, R. A. 1976, *Soviet Astr.*, **20**, 290.
Meyer, F., and Meyer-Hofmeister, E. 1981, *Astr. Ap.*, **104**, L10.
Meyer, F., and Meyer-Hofmeister, E. 1984, *Astr. Ap.*, **140**, L35.
Mineshige, S. 1988, *Astr. Ap.*, **190**, 72.
Mineshige, S., and Osaki, Y. 1983, *Pub. Astr. Soc. Japan*, **35**, 377 (MO83).
———. 1985, *Pub. Astr. Soc. Japan*, **37**, 1.
Mineshige, S., and Shields, G. A. 1990, *Ap. J.*, **351**, 47.
Mineshige, S., and Wheeler, J. C. 1989, *Ap. J.*, **343**, 241.
Osaki, Y. 1974, *Pub. Astr. Soc. Japan*, **26**, 429.
Priedhorsky, W. C., and Holt, S. S. 1987, *Space Sci. Rev.*, **45**, 291.
Priedhorsky, W. C., Terrell, J., and Holt, S. S. 1983, *Ap. J.*, **270**, 233.
Pringle, J. E. 1981, *Ann. Rev. Astr. Ap.*, **19**, 137.
Richtmyer, R. D., and Morton, E. W. 1967, *Difference Methods for Initial-Value Problems*, 2d ed. (New York: Interscience).
Saio, H., Cannizzo, J. K., and Wheeler, J. C. 1987, *Ap. J.*, **316**, 716.
Saito, N. 1990, *Pub. Astr. Soc. Japan*, in press.
Schwarzenberg-Czerny, A. 1989, *Astr. Ap.*, **210**, 174.
Shields, G. A., McKee, C. F., Lin, D. N. C., and Begelman, M. C. 1986, *Ap. J.*, **306**, 90.
Smak, J., 1984, *Acta Astr.*, **34**, 161.
———. 1987, *Ap. Space Sci.*, **131**, 497.
Tuchman, Y., Mineshige, S., and Wheeler, J. C. 1990, *Ap. J.*, **359**, 164 (Paper I).
Tuchman, Y., Sack, N., and Barkat, Z. 1978, *Ap. J.*, **219**, 183.
van Paradijs, J., and Verbunt, F. 1984, in *High Energy Transients in Astrophysics*, ed. S. E. Woosley (AIP Conf. Proc. No. 115), p. 49.
Verbunt, F. 1987, *Astr. Ap. Suppl.*, **71**, 339.
Whelan, J. A. J., *et al.* 1977, *M.N.R.A.S.*, **180**, 657.

S. MINESHIGE: Institute of Astronomy, Madingley Road, Cambridge, CB3 0HA, UK

Y. TUCHMAN: Department of Physics, Hebrew University, Jerusalem, Israel

J. C. WHEELER: Astronomy Department, The University of Texas at Austin, RLM 15.308, Austin, TX 78712-1083

© American Astronomical Society • Provided by the NASA Astrophysics Data System